

ABSTRACTA WROUGHT COBALT-CHROMIUM-MOLYBDENUM ALLOY
FOR SURGICAL IMPLANTS

Thomas M. Devine, Jr.

Submitted to the Department of Metallurgy and Materials Science
on May 14, 1971
in partial fulfillment for the requirements for the Degree of
Bachelor of Science and Master of Science in
Metallurgy and Materials Science

A wrought cobalt-chromium-molybdenum alloy with crevice corrosion resistance identical to that of Vitallium has been developed. The breakdown potential in isotonic salt solution of this new alloy vs. SCE has been measured as 440 mV. Rest potential measurements in isotonic salt solution suggest this M.I.T. alloy to be superior to Vitallium, Haynes Stellite 21, and Haynes Stellite 25. The passive film corrosion rates in isotonic salt solution of the above four alloys are comparable. Through proper working and heat treatment the yield strength of this new alloy can be raised to 125 ksi while maintaining an elongation of 25%. It is suggested that this alloy be used in surgical implants of thin cross-section where the use of precision-cast Vitallium is prevented.

Thesis Supervisor: John Wulff
Title: Professor Emeritus of Metallurgy
and Materials Science

ACKNOWLEDGEMENTS

I wish to thank Mr. Guenther Arndt, Mr. Fred Kummer, and Mr. Peter Wender for their competent assistance throughout the experimental phases of this program.

It is indeed a pleasure to thank my thesis advisor, Professor John Wulff, for his guidance and inspiration during my five years at M.I.T.

Finally, to my wife who typed this thesis for her patience and understanding I am indebted.

TABLE OF CONTENTS

<u>Chapter</u>		<u>Page</u>
	TITLE PAGE	i
	ABSTRACT	ii
	ACKNOWLEDGEMENTS	iii
	TABLE OF CONTENTS	iv
	LIST OF FIGURES	v
	LIST OF TABLES	vii
1	INTRODUCTION	1
2	EXPERIMENTAL	9
	2.1 Corrosion Measurements	10
	2.1.1 Crevice Corrosion Tests	10
	2.1.2 Electrochemical Measurements	11
	2.2 Formability, Mechanical Properties, and Microstructure	12
	2.3 Results	13
3	DISCUSSION AND CONCLUSIONS	21
4	RECOMMENDATIONS FOR FUTURE WORK	24
	REFERENCES	25

LIST OF FIGURES

<u>No.</u>		<u>Page</u>
1	Effect of Cobalt Content on Transformation Temperature of Co-Ni-20Cr-10 Mo Alloys	29
2	Hardness of Co-Cr-Mo Alloys after Heat Treating for 10 Hours at 700°C	30
3	Crevice Corrosion Samples of Several Alloys after Immersion in 10% HCl + 1% FeCl ₃ Solution	31
4	Passive Current Density Vs. Time Curve of 316L Stainless Steel 0.9% NaCl Solution	32
5	Passive Current Density Vs. Time Curve of Hastalloy C in 0.9% NaCl Solution	33
6	Passive Current Density Vs. Time Curve of MP35N in 0.9% NaCl Solution	34
7	Passive Current Density Vs. Time Curve of Haynes Stellite 25 in 0.9% NaCl Solution	35
8	Passive Current Density Vs. Time Curve of Haynes Stellite 21 in 0.9% NaCl Solution	36
9	Passive Current Density Vs. Time Curve of M.I.T. Alloy No. 7 in 0.9% NaCl Solution	37
10	Comparison of the Passive Current Vs. Time Curves of Haynes Stellite 21, Haynes Stellite 25, and M.I.T. Alloy No. 7 in 0.9% NaCl Solution	38
11	Anodic Polarization of 316L Stainless Steel in 0.9% NaCl Solution	39
12	Anodic Polarization of Hastalloy C in 0.9% NaCl Solution	40
13	Anodic Polarization of MP35N in 0.9% NaCl Solution	41
14	Anodic Polarization of Haynes Stellite 25 in 0.9% NaCl Solution	42

<u>No.</u>		<u>Page</u>
15	Anodic Polarization of Haynes Stellite 21 in 0.9% NaCl Solution	43
16	Anodic Polarization of Precision Cast Vitalium in 0.9% NaCl Solution.	44
17	Anodic Polarization of M.I.T. Alloy No. 7 in 0.9% NaCl Solution	45
18	Rest Potentials of M.I.T. Alloy No. 7 and Haynes Stellites 21 and 25 after a 20 Hour Immersion in 0.9% NaCl Solution	46
19	M.I.T. Alloy No. 7. Annealed at 1200°C for 4 Hours and Quenched in Water. 5% HCl Electrolytic Etch. X500	47
20	M.I.T. Alloy No. 7. Directionally Solidified and Extruded. 5% HCl Electrolytic Etch. X500	48
21	M.I.T. Alloy No. 7. Hot and Cold Worked and Heat Treated at 1100°C for 1 Hour and Quenched in Water. 5% HCl Electrolytic Etch. X500	49

LIST OF TABLES

<u>No.</u>		<u>Page</u>
1	Nominal Compositions of Surgical Implant Alloys	50
2	Mechanical Properties of Surgical Implant Alloys	51
3	Strength and Ductility of Co-Base Cr-Mo Alloys at 1700°F	52
4	Room Temperature Ductility of Co-Base Cr-Mo Alloys	53
5	Nominal Compositions of Some Commercially Available Wrought Alloys, Haynes Stellite 21, and Vitallium	54
6	Nominal Compositions of M.I.T. Experimental Alloys	55
7	Mechanical Properties of Some Wrought Commercial Alloys and H.S. 21	56
8	Specifications of Mechanical Properties of Surgical Implant Alloys	57
9	Times to Initiate Crevice Corrosion of Some Commercial Wrought Alloys, H.S. 21, and Vitallium in a 10% HCl + 1% FeCl ₃ Solution at 37°C	58
10	Times to Initiate Crevice Corrosion of M.I.T. Experimental Alloys NO. 1 - 7 in a 10% HCl + 1% FeCl ₃ Solution at 37°C	59
11	Times to Initiate Crevice Corrosion of M.I.T. Experimental Alloys Nos. 7 - 11 in a 10% HCl + 1% FeCl ₃ Solution at 37°C	60
12	Breakdown Potentials in 0.9% NaCl Solution and Rest Potentials After a 20 Hr. Immersion in 0.9% NaCl Solution of H.S. 21, Vitallium, and M.I.T. Alloy No. 7	61

<u>No.</u>		<u>Page</u>
13	Hot and Cold Workability of M.I.T. Alloy No. 7	62
14	Comparison of the Room Temperature Tensile Properties of M.I.T. Alloy No. 7 Following Different Treatments with Those of H.S. 21 and H.S. 25	63

Chapter I

Introduction

Surgical implant material must be corrosion resistant to body fluids and be compatible with body materials. Any ions released must not be harmful to bone, tissue, or fluids. The implants must also have the required strength, ductility, fatigue resistance, and in parts where the implant rubs against itself or tissue and bone, the material must have the proper coefficient of friction to avoid wear and tissue inflammation.¹

Four metallic alloy systems are now used as surgical implant material. They are molybdenum containing wrought, austenitic stainless steel (316, 316L), precision cast cobalt-chromium-molybdenum alloys (Vitallium, Haynes Stellite 21, Vinertia), a wrought cobalt-chromium-tungsten-nickel alloy (Haynes Stellite 25), and commercial, wrought, unalloyed titanium. The compositions and mechanical properties of these alloys are listed in Tables 1 and 2, respectively. Unfortunately, none of the above alloys can be regarded as ideally suitable implant material. Stainless steel tends to pit and crevice corrode in body fluids.^{2,3,4,5,6} While precision cast cobalt-chromium-molybdenum-carbon alloys have superior corrosion resistance, they possess insufficient ductility to overcome shortcomings in design or fabrication.⁷ The latter alloys can only be hot worked with extreme care^{8,9} and yet thin sections are difficult to cast without incurring harmful structural defects.¹⁰ For these reasons the wrought alloy Haynes Stellite 25 is often used as a substitute in thin-section implants. Although it possesses admirable mechanical properties, Haynes Stellite 25 is susceptible to crevice corrosion in body fluids.^{11,12,13} It nevertheless

appears to be far more resistant to all forms of corrosion than austenitic stainless steels.¹⁴ Ordinary commercial titanium and some of its alloys while exhibiting superior long-time corrosion resistance¹⁵ in body fluids relative to all of the above alloys possesses little wear resistance and a high coefficient of friction when in rubbing contact with itself, for example, in articulating prosthesis. Although its corrosion products do not irritate the tissues of animals and, presumably of humans, as much as any of the other currently used alloys,¹⁵ they do stain the adjacent tissue black. This has not as yet been found harmful^{15,16,17} and does not seem to disturb foreign surgeons but does prevent the American surgeons from accepting titanium as surgical implant material. To reduce the initial rate of corrosion of titanium and its alloys and thus eliminate tissue stains as well as to improve their wear-corrosion resistance has been one of the goals of our laboratory at M.I.T. The progress achieved thus far with titanium will be reported in a forthcoming M.I.T. M. S. Thesis.¹⁸ The present thesis is, however, concerned with the development of a new cobalt-chromium-molybdenum alloy with possible immediate acceptability, superior resistance to all forms of corrosion, and hot as well as cold workability.

The first noteworthy cobalt-chromium base alloys which received considerable attention due to their high corrosion and wear resistance were the cast cobalt-chromium-tungsten-high carbon alloys patented in 1907 by Elwood Haynes.¹⁹ Erdle²⁰ patented a cobalt-chromium-tungsten-carbon alloy containing higher tungsten but lower carbon contents suitable for investment casting of surgical implants and other small, intricate-shaped parts. Molybdenum was later substituted for tungsten

in this alloy by Erdle and Prange²¹. During World War II, it was found that the investment casting technique lent itself to the manufacture of heat resistant parts, and Erdle and Prange's cobalt-chromium-molybdenum-low carbon alloy modified by additions of 3 - 5% nickel became the most popular heat resistant alloy. This modified alloy has become known in the literature as Haynes Stellite 21.

Most of the published data regarding the processing and mechanical properties of cobalt-chromium-molybdenum-base alloys can only be gleaned from the writings of workers interested in high-temperature applications rather than corrosion resistance. Nevertheless, a significant amount of information concerning the physical metallurgy of cobalt-chromium-base alloys is attainable from these works. The matrix phase of cobalt-rich alloys has been shown by a number of authors^{22,23,24,25} to undergo a high temperature transformation reaction from the face-centered cubic to the hexagonal close-packed structure. The transformation temperature, as depicted in Fig. 1, was determined by Smith and Yates²² to vary with the cobalt content of the alloy. Increasing the cobalt content progressively raised the transformation temperature. In pure cobalt, the transformation from the face-central cubic to the hexagonal close-packed structure was shown by Troiano and Tokich²⁶ to occur by a martensitic type reaction. Weeton and Signorelli²⁴ assumed the same type of transformation reaction to occur in the matrix phase of cobalt-rich, chromium-molybdenum-nickel alloys.

The birth and growth of jet propulsion spurred the development of a number of cobalt-chromium base alloys. The processing,

high-temperature properties, and development of such alloys are well reviewed in a publication of the Metallurgical Society Conferences.²⁷ Especially pertinent to this thesis is a paper, included in the above work, by Rausch, McAndrew, and Simcoe.²⁸ These authors primarily investigated the effects of alloying wrought cobalt-chromium base alloys with additions of molybdenum, tungsten, and tantalum. If considered on a weight percentage basis, molybdenum was the most potent strengthener. To maintain forgeability at high chromium levels (> 20% Cr) the authors had to maintain the molybdenum content at a low level as indicated in Table 3, which lists the high-temperature ductilities of a number of cobalt-chromium-molybdenum alloys. Table 4 lists the room temperature ductilities of these same alloys; the results indicate that to maintain cold workability at high chromium levels, the molybdenum content must be kept low.

In addition to the workability of cobalt-chromium base alloys, several authors have investigated the age-hardening characteristics of these alloys. Drapier et al²⁵ found that a solution treatment of a 13 Mo - 17 Cr - Bal Co alloy at 1200°C for 1000 hours followed by a water quench and subsequent aging at 800°C for 1 hour produced a precipitate-free hexagonal-close-packed matrix. Aging for 20 and 100 hours precipitated the (Cr, Mo, Co) R phase.²⁵ Drapier and co-workers,²⁵ as well as Lux and Bollman²⁹ found that aging of an 11 Cr - 14 Mo - Bal Co alloy at 700°C for 2 and 20 hours produced a thread-like precipitate suggested by the latter investigators to be either Co_3Mo (hexagonal, ordered) or Co_7Mo_6 (μ phase, rhombohedral-hexagonal). Although the nature of the phases responsible for the hardening in cobalt-rich,

chromium-molybdenum alloys has not yet been clearly established, Drapier and co-workers,²⁵ as shown in Fig. 2, have demonstrated the significant increases in hardness produced by aging treatments.

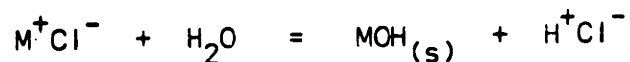
Dilute additions of carbon to cobalt base Cr - Ni - Mo alloys such as Haynes Stellite 21 greatly complicates matters. A number of samples of Haynes Stellite 21 containing 0.29 C were solution treated by Weeton and Signorelli²⁴ at 1230°C for 72 hours and then either water-quenched and aged or held at lower temperatures for isothermal transformations. Isothermal transformations of the solution-treated material at temperatures of 1065°C and 955°C resulted in the formation of a lamellar, pearlitic type of precipitate, possibly of $Cr_{23}C_6$ and or M_6C . There was also evidence of σ phase formation. The precipitate formed during the isothermal treatment at 815°C was almost entirely of a Widmanstätten type distributed throughout the grains. In sharp contrast to the precipitates formed during isothermal transformation, aging at 1065°C, 955°C, and 815°C resulted in precipitation almost entirely along slip lines and twin boundaries which formed during the quenching operation. The temperature for development of the maximum hardness in the solution treated material was between 760°C and 815°C. Aging for 72 hours in this temperature range produced a hardness of R_c 42. The maximum hardness for the isothermal transformation was R_c 40 and was developed between 815°C and 870°C.²⁴

As was mentioned in reference to workability, cobalt-chromium base alloys are considered as high temperature alloys in the literature. Hence, most of the corrosion data on these alloys are for temperatures of 600°C and above. Nevertheless, several investigations^{30,31,32} have

been reported on the corrosion behavior of cobalt-chromium base alloys at room and body temperatures in chloride-ion containing environments. From rest potential measurements, the most noble cobalt-chromium binary alloy was determined by Greener et al³¹ to contain 25% chromium. Hoar and Mears³⁰ reported Vitallium to possess corrosion resistance superior to any of the nickel base alloys and stainless steels which they examined. The latter authors further report that the difference in breakdown potential and rest potential of Vitallium after 200 days in a .17 M solution of sodium chloride is so large (0.37 v) that passive film breakdown of Vitallium in this solution is highly unlikely. Hoar and Mears also indicate that as the concentration of sodium chloride in the solution is increased from 0.17 M to 1 M, the breakdown potential of Vitallium decreases by approximately 0.5 v. It is a well-documented fact^{33,34,35} that in pits and crevices a significant build-up in chloride ion content can occur. Such an increase in chloride-ion content, as described below, can affect a breakdown in passivity and localized corrosion will occur in the pit or crevice. Because most of the implants employed by surgeons inherently contain crevices due to implant-bone, implant-screw, and screw-bone areas of contact, implant material should be highly resistant to crevice as well as general corrosion. In this thesis, implant material was therefore tested for general, pit, and crevice corrosion resistance.

Due to the above mentioned importance of crevice corrosion in surgical implants, a brief discussion of the mechanism of crevice corrosion, following the treatment of Greene and Fontana,³⁵ may be of assistance to the reader. The surface of a metal or alloy containing

holes, crevices, or other such surface irregularities which can accommodate small volumes of stagnant solution may undergo intense localized corrosion within the surface defects. This form of corrosion is termed crevice corrosion. A number of experiments^{36, 37, 38, 39} within the past ten years have questioned the theories which attributed crevice corrosion to differences in metal ion or oxygen concentration between the crevice and its surroundings. The basic mechanism of crevice corrosion may be illustrated by considering a riveted plate section of iron or steel immersed in aerated sea-water. The reaction involves the dissolution of metal along with the reduction of oxygen to hydroxide ions. Initially, the two reactions occur uniformly over the entire surface, including the interior of the crevice. After a short period of time, the solution within the crevice is depleted of oxygen because of restricted convection, and oxygen reduction ceases in this area. The dissolution of metal in this area continues while oxygen reduction has ceased. This produces an excess of positive charge in the solution, promoting the migration of chloride ions into the crevice.^{40, 41, 42} The result is an increase in the concentration of metal chloride within the crevice. With the exception of the alkali metals, metal salts such as chlorides hydrolyze in water:



An aqueous solution of a metal chloride dissociates into an insoluble hydroxide and a free acid. Both chloride and hydrogen ions accelerate the dissolution rates of most metals and alloys.³⁵ These are both present in the crevice due to migration and hydrolysis, and there

results an increase in the dissolution rate of the metal. This increase in dissolution in turn increases migration of the chloride ions into the crevice,^{40,41,42} and the entire process becomes autocatalytic.^{40,43} The fluid within crevices exposed to dilute neutral sodium chloride solutions has been found to possess a pH of 2 to 3.³⁵ In stainless steel crevices, the potential is 0.55 - 0.60 v more active than that outside the crevice.³⁴

Due to the reported crevice corrosion susceptibility of Haynes Stellite 25 in body fluids,^{11,12,13} and the insufficient ductility of Vitallium,⁷ of immediate need is an alloy which has the corrosion resistance of Vitallium and can be hot and cold worked. Should such an alloy be developed, the beneficiary would be mankind.

Chapter 2

EXPERIMENTAL

The primary concerns of the bio-materials engineer are the corrosion resistance and mechanical strength of surgical implants. Associated with the former, and of vital importance to the surgeon and patient, is compatibility of the corrosion products with the body materials. Coupled with mechanical strength is ease of formability which is of special significance to the fabricator.

Although Vitallium has excellent corrosion resistance in body fluids,⁴⁴ its use as surgical implant material is severely restricted. The less than adequate high temperature ductility of Vitallium demands that a great deal of care and attention be given to hot working operations. Similarly, the low, room temperature ductility of Vitallium prevents any reasonable amount of cold working. As a result, Vitallium is employed only in those parts which need be precision cast. Because castings of thin-section implants have insufficient mechanical strength, a wrought cobalt-chromium-tungsten-nickel alloy, Haynes Stellite 25, has been used in such parts in place of Vitallium. However, with the reported susceptibility of Haynes Stellite 25 to crevice corrosion in body fluids,^{11,12,13} a new alloy which can be both hot and cold worked and which possesses a corrosion resistance comparable to Vitallium appears to be required.

With the goal of finding such an alloy, a number of commercially available, wrought alloys, listed in Table 5, were tested for crevice corrosion resistance. In addition, eleven alloys made in our

laboratory at M.I.T., and listed in Table 6, were prepared in an arc-melter with a water-cooled copper hearth and tested for hot and cold workability as well as corrosion resistance.

2.1 Corrosion Measurements

2.1.1 Crevice Corrosion Tests

Because of the crevices inherent in surgical implants installed in the body, it was decided to test the currently used and potentially usable surgical implant materials listed in Tables 5 and 6 for susceptibility to crevice corrosion. After a mechanical polish to 4/0 grit paper, cylindrical specimens nominally 0.25" in diameter x 1" in length were fitted with teflon gaskets nominally 0.125" in width and 0.015" smaller in diameter than the samples and immersed in various corrosive media. Because of the high corrosion resistance of these alloys, accelerated solutions were employed so that results could be obtained in a reasonable length of time. These tests were conducted in a 10% (by weight) HCl + 1% FeCl₃ solution. Three different test temperatures were also employed, room temperature, body temperature (37.5°C), and 50°C. The crevice corrosion tests were conducted in an incubator which maintained the temperature of the system constant. The alloys were rated on their resistance to crevice corrosion by the lengths of time required to produce visible crevice corrosion. The onset of crevice corrosion was indicated by both discoloration of the test solution and the evidence of corrosion occurring in the material at the rim of the teflon gasket. General corrosion tests in the accelerated solutions were also performed on cylindrical-shaped

specimens of these alloys and the corrosion rates were measured by weight loss of the specimen and expressed as inches of penetration per year, ipy.

2.1.2 Electrochemical Measurements

Corrosion rates of implant materials in body fluids must be extremely low in order to avoid inflammation and toxicity of adjacent fluids and tissues. In fact, the corrosion rates must be so low that it is impossible to determine them by weight loss measurements. For measuring the low corrosion rates of highly corrosion resistant alloys, it is necessary to employ electrochemical techniques. These are of two kinds. One called the linear polarization technique^{44,45} and the other, the one employed in this thesis, called the passive current-time technique.⁴⁵ The benefit of the passive current-time technique, which was developed by Vetter,⁴⁶ is that continuous measurements of the corrosion rate can be obtained from the instant the specimen is immersed in the solution.

Implants, especially those made of 316 stainless steel, are susceptible to pit corrosion. Although the initiation mechanisms of pit and crevice corrosion may be different,^{36,37,38} crevice corrosion in passive metals and alloys and pit corrosion are both related to the breakdown of the passive film in localized areas on the specimen surface.^{34,35} The pitting potential is usually measured by potentiostatically polarizing the specimen as an anode until the anodic current sharply increases, indicating the breakdown of passivity and the onset of pitting.

As mentioned by Hoar and Mears,³⁰ the stability of the passive film is indicated by the difference in potential of the material in the corrosive medium and the breakdown potential of the material in that same environment. The potential of a material in a corrosive medium can be measured by the potential-time, or, rest potential technique, whereby a specimen is immersed in an aerated corrosive solution and its potential is determined as a function of time. Rest potential experiments were performed on a number of the alloys listed in Tables 5 and 6.

Each cylindrically-shaped specimen used in the electrochemical tests was mechanically polished to 4/0 grit and then drilled and tapped to fit into a stainless steel rod, used as a support as well as current lead. As described by Greene,⁴⁸ the latter was enclosed in a glass tube, and a teflon grommet between the glass tube and the specimen maintained a waterproof seal. After assembling the specimen in the electrode holder, the specimen was degreased ultrasonically in trichloroethylene for about ten minutes. The specimen was then rinsed with acetone, distilled water, and, finally, isotonic salt solution (0.9 wt.% NaCl), the test electrolyte.

To remove oxygen from the test solution during the experiment, deoxygenated and dehumidified nitrogen was passed through the testing solution continuously at a rate of 0.5 SCFH (standard cubic foot per hour) as illustrated by Han Shih.⁴⁹

2.2 Formability, Mechanical Properties, and Microstructure

Due to the wide variation in the shapes and designs of surgical implants, the fabricability of surgical implant material is of particular

importance. Those alloys which exhibited superior corrosion resistance in the corrosion tests described above were subjected to various forms of hot and cold working. In order to determine the workability of large, industrial size ingots of the above alloys, various forms of hot and cold working techniques were performed under our instructions at several industrial laboratories. Hammer forging, press-forging, and hot rolling experiments were conducted at the Haynes Stellite laboratory in Kokomo, Indiana; additional hot rolling experiments were conducted at the International Nickel Company, Research Laboratory in Sterling Forest, New York, and Whitaker Corporation of Concord, Massachusetts performed several extrusion operations. Cold rolling and cold swaging experiments were performed here at M.I.T.

Mechanical properties of the various alloys were tabulated in terms of hardness and tensile data. Hardness experiments utilized a Tykon Hardness Indenter Machine while tensile data was accumulated with the aid of an Instron Testing Machine using a 20,000 lb-F cell and an 0.02 min^{-1} cross-head speed.

A General Electric Diffractometer was employed to investigate the nature of the phase or phases present in various alloys. Photomicrographs supplied information on the distribution and morphology of the phases existent in various alloys.

2.3 Results

Table 7 lists the room temperature tensile properties and hardness data of a number of commercially available, corrosion resistant, wrought materials. The chemical compositions of these alloys

have already been cited in Table 5. Included in Table 7 for the purpose of comparison are the tensile and hardness data of Haynes Stellite 21 and Vitallium. These results indicate that 316L stainless steel in the cold-worked form and the other remaining alloys meet the mechanical specifications for surgical implant materials set by ASTM Committee F-4,⁵⁰ listed in Table 8, and are vastly superior to Haynes Stellite 21 and Vitallium.

Because of the autocatalytic nature of crevice corrosion,^{34,35,37} the most significant parameter in rating an alloy's susceptibility to crevice corrosion is the time required to initiate this form of corrosion. Hence, in testing the crevice corrosion resistance of the commercial, wrought alloys referred to above, the times required for the onset of visible crevice corrosion in the accelerated crevice corrosion test described in Section 2.1.1 were recorded. Table 9 compares the incubation periods for crevice corrosion initiation of Haynes Stellite 21 and Vitallium with those of the commercial wrought alloys. As indicated in this table the crevice corrosion resistance of any of the wrought alloys is vastly inferior to that of Vitallium. In particular, 316L stainless steel, an alloy which still finds use as surgical implant material, by far exhibits the least crevice corrosion resistance of all the alloys tested. Figure 3 vividly depicts the extent of the crevice attack of the various wrought alloys after various immersion times in a solution of 10% HCl + 1% FeCl₃. The crevice corrosion damage varies from severe deep grooving of 316L stainless steel after less than one day immersion to a slight scar on

on the surface of Hastalloy C after an eleven day immersion. Of particular interest is the large difference in crevice corrosion resistance between Haynes Stellite 21 and Vitallium. Evidently the small amount of nickel + iron (<5%) found in Haynes Stellite 21 severely limits its crevice corrosion resistance.

The unfortunate lack of a commercial, wrought alloy with crevice corrosion resistance, comparable to that of Vitallium prompted the preparation of eight experimental alloys in our laboratory. These alloys were produced by employing an arc melter as described in the introduction of Chapter 2. Their compositions have already been reported in Table 6. The results of the accelerated crevice corrosion test on these alloys are reported in Table 10. These results illustrate two points. The M.I.T. alloys No. 1, 2, and 3 indicate an optimum chromium-molybdenum ratio of 2:1 in cobalt-nickel base alloys where the chromium + molybdenum content is a constant equal to 30%. The M.I.T. alloys No. 2, 4, 5, 6, and 7 reveal a most interesting fact. As the nickel content is decreased from 35% to 0% while the chromium and molybdenum contents are held constant, the crevice corrosion resistance of the cobalt-base alloys progressively increases as indicated by the increase in the time to produce visible crevice corrosion from 5 to 8 days (M.I.T. alloy No. 2) to > 280 days (M.I.T. alloy No. 7). This latter result would seem to indicate that the 2.5% nickel content of Haynes Stellite 21 is responsible for the alloy's high susceptibility to crevice corrosion as compared to Vitallium. Further attempts to refine the optimum amounts of chromium and molybdenum in a cobalt-base

alloy were attempted. M.I.T. alloys No. 8 - 11, whose compositions are also listed in Table 6, were prepared. Although M.I.T. alloy No. 8 exhibited the same crevice corrosion resistance in the accelerated solution as M.I.T. alloy No. 7, M.I.T. alloys No. 9, 10, and 11 demonstrated decreasing resistance to crevice corrosion as indicated in Table 11.

The crevice corrosion results of M.I.T. alloys No. 7 and 8 seemed so promising that cold swaging experiments were conducted on each alloy to determine their cold workability. Rods of each of the two alloys were therefore prepared, annealed at 1200°C for 4 hours, quenched in water, and cold swaged. A 30% reduction in area was achieved with M.I.T. alloy No. 7 before surface cracking occurred whereas a similar state was reached in M.I.T. alloy No. 8 after only a 10% reduction in area. These preliminary crevice corrosion and cold working experiments indicated that further efforts should be devoted to exploring the corrosion resistance and workability of M.I.T. alloy No. 7.

In order to compare the corrosion rates of Haynes Stellite 21, and the commercial, wrought alloys to that of M.I.T. alloy No. 7, passive current tests, as described in section 2.12, were conducted in isotonic salt solution (0.9 wt. % NaCl). The results for the above alloys are shown in Figures 4 to 9. Figure 10 is a compilation of Figures 7, 8, and 9 and illustrates that after 500 minutes in the test electrolyte, alloy No. 7 exhibits the same low rate of passive film corrosion as Haynes Stellites 21 and 25.

To obtain the value of the breakdown potential of an alloy, the anodic polarization test, described in section 2.1.2, was performed in deaerated isotonic salt solution. The curves for 316L stainless steel, MP35N, Hastalloy C, Haynes Stellite 21, Haynes Stellite 25, Vitallium, and M.I.T. alloy No. 7 are shown in Figures 11 to 17. They show the active-passive transitions. The breakdown potential with respect to the potential of standard calomel cell employed in the case of 316L stainless steel was 300 millivolts, that found for Vitallium, 340 mV, for Haynes Stellite 21, 360 mV, for Haynes Stellite 25, 370 mV, for Hastalloy C, 425 mV, for M.I.T. alloy No. 7, 440 mV, and MP35N, 460 mV. All these alloys exhibited visible evidence of pitting after the above breakdown potentials were exceeded in the test. The values obtained for such potentials are in accord with those of Han Shih⁴⁹ for 316L stainless steel, Haynes Stellite 21, and Haynes Stellite 25.

As indicated by Hoar and Mears,³⁰ the resistance to pit and crevice corrosion of an alloy may be ascertained by comparing the potential of the alloy immersed in solution with the breakdown potential of the alloy in the same solution. The lower the value of the rest potential as compared with the breakdown potential, the greater is the pit and crevice corrosion resistance of the alloy. Han Shih⁴⁹ indicates that the potential of 316L stainless steel increases steadily with time of exposure in the corrodent and presumably approaches within a relatively short time a value equivalent to its breakdown potential. Table 12 lists the breakdown potentials of Haynes Stellite 21, Vitallium, and M.I.T. alloy No. 7 along with their rest potentials recorded after a 20 hour immersion in isotonic salt solution. Column 4 of this table

indicates that M.I.T. alloy No. 7 by far exhibits the greatest difference between the breakdown and rest potentials, implying that alloy No. 7 should have the strongest resistance to pit and crevice corrosion in isotonic salt solutions of the three alloys tested.

Figure 18 is a photomicrograph of M.I.T. alloy No. 7 after an annealing treatment at 1200°C for 4 hours followed by a water quench. X-ray diffraction experiments utilizing chromium radiation of M.I.T. alloy No. 7 in the above condition indicate the alloy to be composed of a precipitate-free, face centered cubic matrix. Figure 19 shows the microstructure of an extruded sample of a directionally solidified ingot of M.I.T. alloy No. 7. Due to the pronounced texture present in the latter form of M.I.T. alloy No. 7 it was impossible to determine the fraction of matrix present as face-centered cubic and that existing in the hexagonal close-packed structure. The strongest line present in the diffraction spectrum corresponded to diffraction off the (10·1) planes. There was also evidence of the presence of the (Cr, Mo, Co) R phase.

Despite the superior corrosion resistance of M.I.T. alloy No. 7, it will be of little assistance to the orthopedic surgeon and patient unless it lends itself to hot and cold working treatments. Arc melted ingots of M.I.T. alloy No. 7 were annealed at 1200°C for 4 hours and quenched in water. Standard axisymmetric tensile samples, 1-1/4" gauge length x 1/4" diameter, were then machined and pulled in tension. These samples exhibited an 0.2% offset yield strength of 45 ksi, an ultimate tensile strength of 55 ksi, an elongation of 20% and a reduction in area of 26%. When aged at 800°C for one hour and quenched in water,

M.I.T. alloy No. 7 had an 0.2% offset yield strength of 55 ksi, an ultimate tensile strength of 115 ksi, an elongation of 10% and a reduction in area of 12%. When the annealing treatment is followed by cold swaging to 25% reduction in area, the yield strength is increased to 94 ksi, the ultimate tensile strength to 138 ksi, but the elongation and reduction in area are both lowered to 2%.

A directionally solidified ingot of M.I.T. alloy No. 7 was successfully extruded to a 64% reduction in area. Axisymmetric tensile samples machined from the above bar exhibited a yield strength of 110 ksi, an ultimate tensile strength of 134 ksi, and elongation of 5.2%, and a reduction in area of 15%. When the directionally solidified, as-extruded ingot was heat-treated at 900°C for 1/2 hour, a yield strength of 117 ksi, an ultimate tensile strength of 134 ksi, an elongation of 6.5%, and a reduction in area of 19% were obtained. Annealing at 1000°C for one hour, quenching in water than then annealing at 1100°C for one hour and quenching in water produced a yield strength of 72 ksi, an ultimate tensile strength of 142 ksi, an elongation of 9%, and a reduction in area of 38%.

In addition, a 10 lb. 3" diameter x 5" cylindrical ingot of M.I.T. alloy No. 7 was press forged to a 83% reduction in area, hot rolled to a 64% reduction in area, and then cold swaged to a 25% reduction in area, producing a hardness of $R_c 44$. When tensile samples from the above stock were heat treated at 1100°C for one hour, quenched in water and pulled, they exhibited a yield strength of 125 ksi, an ultimate tensile strength of 206 ksi, an elongation of 25% and a reduction in area of 26%. The microstructure of M.I.T. alloy No. 7

resulting from the above hot and cold working and heat treatment is revealed in Figure 20. X-ray diffraction analysis of the above sample indicates the matrix to be composed of both face centered cubic and hexagonal close-packed phases. X-rays also revealed the presence of carbide precipitation in the form of Cr_7C_3 and MoC . Tables 13 and 14 summarize the hot and cold workability and room temperature mechanical properties of respectively of M.I.T. alloy No. 7. Table 14 also includes the mechanical properties of Haynes Stellite alloys 21 and 25 for the purpose of comparison.

Chapter 3

DISCUSSION AND CONCLUSIONS

Despite the well-known increases in toughness derived from additions of nickel to cobalt-base alloys, the deleterious effect of nickel on the crevice corrosion susceptibility of these alloys prevented even dilute additions of this element. The exact nature of the role nickel plays in reducing the crevice corrosion resistance of cobalt-chromium-molybdenum alloys is not clearly understood. G. D. Smith²³ has also reported this detrimental effect of nickel.

Although Acharya et al³¹ found the brittle σ phase present in 30 Cr-Co binary alloys but absent in 25 Cr-Co binary alloys, Beck and co-workers⁵¹ determined that in the chromium-molybdenum-cobalt system at 1200°C the (Cr-Co) σ phase formed an elongated field of ternary solid solutions suggesting that molybdenum is capable of partially replacing chromium in forming the σ phase. This would explain the brittle behavior of M.I.T. alloy No. 8 (25 Cr-5Mo) relative to M.I.T. alloy No. 7 (20 Cr-10 Mo).

Although M.I.T. alloy No. 7 cannot be hot or cold worked as readily as Haynes Stellite 25, the forging (83%RA), hot rolling (64%RA), and extrusion (64%RA) experiments on the former alloy demonstrate the more than adequate hot workability of this alloy. Furthermore, the 25% cold reductions in area obtained by swaging and rolling M.I.T. alloy No. 7 indicate a significant degree of cold workability. With the proper thermomechanical and cold working history followed by the 1100°C for one hour heat treatment, the ductility (25% elongation) of

M.I.T. alloy No. 7 begins to rival that of Haynes Stellite 25 (35% elongation), while the strength of the former greatly exceeds that of the latter.

The crevice corrosion resistance as measured by initiation time in accelerated tests of M.I.T. alloy No. 7 (>280 days) is far superior to that of Haynes Stellite alloys 21 (14-22 days) and 25 (6-12 days) and is identical to that of Vitallium. Furthermore, the results of the anodic polarization and rest potential tests show M.I.T. alloy No. 7 to be superior to both Haynes Stellite alloys 21 and 25 as well as Vitallium. Finally, the passive film corrosion rates of Haynes Stellite 21, Haynes Stellite 25, Vitallium and M.I.T. alloy No. 7 are comparable.

As a precision casting alloy Vitallium is definitely superior to M.I.T. alloy No. 7 because of the low-as-cast strength of the latter alloy. This can however be ameliorated by additions of 0.2 - 0.3% carbon to the M.I.T. alloy. To prevent the formation of $Cr_7 C_6$ and MoC in this high carbon version of M.I.T. alloy No. 7 which would deplete the matrix area surrounding these precipitates of chromium and molybdenum and result in an overall reduction in the corrosion resistance of the alloy, sufficient additions of titanium and niobium could be made to tie up the carbon as TiC or NbC .

From preliminary wear experiments not reported in this thesis, fully hardened Haynes Stellite 25 was found to be less resistant to adhesive wear than cast Vitallium of a similar hardness. The cast, high carbon version of M.I.T. alloy No. 7 exhibited wear resistance quite similar to Vitallium. For articulating prostheses neither

Vitalium nor M.I.T. alloy No. 7 are wholly satisfactory. On this account we are currently experimenting with plasma-jet sprayed coatings on M.I.T. alloy No. 7 containing much higher percentages of titanium, niobium and tungsten carbides.

In summation, the objective to develop a wrought cobalt-chromium-molybdenum alloy with suitable mechanical properties and crevice corrosion resistance superior to that of Haynes Stellite 25 and comparable to that of Vitalium has been realized.

Chapter 4

RECOMMENDATIONS FOR FUTURE WORK

1. Since the accelerated crevice corrosion tests failed to distinguish the relative susceptibilities of Vitallium and M.I.T. alloy No. 7 to this form of corrosion, anodic polarization and rest potential tests of these two alloys should be conducted in solutions of higher chloride-ion content and lower pH to determine which alloy has the greater resistance to crevice corrosion. These tests are being conducted at present.
2. Adhesive and corrosive wear tests of M.I.T. alloy No. 7 in both wrought and cast (0.3%C) forms with and without plasma jet sprayed carbide surfaces should be conducted. These tests are currently being carried out.
3. Prepassivation treatments of M.I.T. alloy No. 7 and Vitallium to lower their initial rates of corrosion have been carried out but not reported in this thesis. Further investigations into this area are also being conducted at this time.
4. Corrosion fatigue studies of M.I.T. alloy No. 7 should be undertaken and compared with such of cast Vitallium. The material for such studies is now being fabricated for us by the Haynes Stellite Division of Union Carbide Corporation.

REFERENCES

1. F. R. Morral, "Cobalt Alloys as Implants in Humans," Journal of Materials, Vol. 1, No. 2, 1966, p. 384.
2. J. T. Scales, G. D. Winter, and H. T. Shirley, "Corrosion of Orthopaedic Implants," Journal of Bone and Joint Surgery, Vol. 41-B, 1959, p. 810.
3. J. H. Hicks and W. H. Cater, "Minor Reactions Due to Modern Metal," Journal of Bone and Joint Surgery, Vol. 44B, No. 1, 1962, p. 122.
4. J. Brettle, United Kingdom Atomic Energy Authority Report No. GRO/44/83/13 (Ex), AWRE Metallurgy Division.
5. F. W. Bultitude and J. R. Morris, United Kingdom Atomic Energy Authority Report No. GRO/44/83/22(Ex).
6. V. J. Colangelo and N. D. Greene, "Corrosion and Fracture of Type 316 SMO Orthopedic Implants," Report to National Institute of Health (GM-12661-01), 1968.
7. K. Asgar and F. A. Peyton, "Effect of Casting Conditions on Some Mechanical Properties of Cobalt Base Alloys," Journal of Dental Research, Vol. 40, No. 1, 1961, p. 73.
8. Personal Communication, April 1971, Forging Master, General Electric Company.
9. Personal Communication, April 1971, S. Wlodek, Union Carbide Corporation, Stellite Division, Kokomo, Indiana.
10. J. M. Zarek, "Biomechanical Appraisal of Metallic Osteosynthesis," Metals and Materials, May, 1967, p. 139.
11. J. Wulff and J. Cohen, "Failure by Crevice Corrosion of Cobalt-Chromium Alloys in Surgical Implants, and a New Cobalt-Chromium Alloy with Superior Properties," Presented at the Nov. 17, 1970, Annual Conference on Engineering in Medicine and Biology, Washington, D. C.
12. G. Arndt, T. M. Devine, and J. Wulff, "A New Cobalt-Chromium-Molybdenum Wrought Alloy," Presented at the Fall Meeting of the Metallurgical Society of AIME, October 19-22, 1970, Cleveland. To be published in Metallurgical Transactions.

13. R. M. Rose, A. Schiller, and E. Radin, "Corrosion-Accelerated Mechanical Failure of a Vitallium Nail-Plate," Submitted to The Journal of Bone and Joint Surgery.
14. Multiphase MP35N Technical Data, published by Latrobe Steel Company, Latrobe, Pennsylvania.
15. P. G. Laing, A. B. Ferguson, and E. S. Hodge, "Tissue Reaction in Rabbit Muscle Exposed to Metallic Implants," Journal of Biomedical Materials Research, Vol. 1, No. 1, 1967, p. 135.
16. H. Emneus, U. Stenram, and I. Baecklund, "An X-Ray Spectrographic Investigation of the Soft Tissue Around Titanium and Cobalt Alloy Implants," Acta Orthopaedica Scandinavica, Supplementum 44A, 1961, p. 3.
17. H. Emneus and U. Stenram, "Reaction of Tissues to Alloys Used in Osteosynthesis," Acta Orthopaedica Scandinavica, Vol. 29, No. 4, 1960, p. 315.
18. F. Kummer, "Titanium Alloys for Surgical Implants," M.I.T. M.S. Thesis, Submitted May 14, 1971.
19. E. Haynes, U. S. Patent 873,745, 1907.
20. C. H. Prange, U. S. Patents, 1,909,008 (1933); 1,958,466 (1934); 2,135,600 (1938); 2,180,549 (1939).
21. R. W. Erdle and C. H. Prange, U. S. Patent 1,956,278 (1934).
22. G. D. Smith, and D. H. Yates, "High Strength, Ductility, Corrosion Resistance: Multiphase Alloys Have All Three," Metal Progress, March, 1968, p. 100.
23. G. D. Smith, U. S. Patent 3,356,542.
24. J. W. Weeton and R. A. Signorelli, "Effect of Heat Treatment Upon Microstructures, Microconstituents, and Hardness of a Wrought Cobalt Base Alloy," Transactions of the American Society of Metals, Vol. 47, 1954, p. 815.
25. J. M. Drapier, J. L. de Brouwer, and D. Coutsouradis, "Refractory Metals and Intermetallic Precipitates in Cobalt-Chromium Alloy," Cobalt, No. 27, 1965, p. 1.
26. A. R. Troiano and J. L. Tokich, "The Transformation of Cobalt," Transactions, American Institute of Mining and Metallurgical Engineers, Vol. 175, 1948, p. 728.

27. G. M. Ault, W. F. Barclay, and H. P. Munger, editors, High Temperature Materials II, Metallurgical Society Conferences, Vol. 18, J. Wiley and Sons, (New York), 1963.
28. J. J. Rausch, J. B. McAndrew, and C. R. Simcoe, "Effect of Alloying on the Properties of Wrought Cobalt," Ibid, p. 259.
29. B. Lux and W. Bollmann, "Precipitation Hardening of Co-Base Alloys by Means of an Intermetallic Co-Mo Phase," Cobalt, No. 11, 1961, p. 4.
30. T. P. Hoar and D. C. Mears, "Corrosion-Resistant Alloys in Chloride Solutions: Materials for Surgical Implants," Proceedings of the Royal Society (London), Vol. A294, 1966, p. 486.
31. A. Acharya, E. Freise, and E. H. Greener, "Open-Circuit Potentials and Microstructure and Some Binary Co-Cr Alloys," Cobalt, No. 47, 1970, p. 75.
32. R. W. Revie and N. D. Greene, "Corrosion Behavior of Surgical Implant Materials: I. Effects of Sterilization," Corrosion Science, Vol. 9, 1969, p. 755.
33. I. L. Rosenfeld and I. S. Danilov, "Electrochemical Aspects of Pitting Corrosion," Corrosion Science, Vol. 7, 1967, p. 129.
34. H. H. Uhlig, Corrosion and Corrosion Control, J. Wiley and Sons, Inc., New York, 1963.
35. M. G. Fontana and N. D. Greene, Corrosion Engineering, McGraw-Hill, New York, 1967.
36. G. J. Schafer and P. K. Foster, "The Role of the Metal-Ion Concentration Cell in Crevice Corrosion," Journal of the Electrochemical Society, Vol. 106, 1959, p. 468.
37. G. J. Schafer, J. R. Gabriel, and P. K. Foster, "On the Role of the Oxygen Concentration Cell in Crevice Corrosion and Pitting," Transactions of the Electrochemical Society, Vol. 12, 1960, p. 1002.
38. Y. M. Korovin and I. B. Ulanovskii, "Effect of Oxygen Concentration and pH on Electrode Potential of Stainless Steels and Operation of Microcouples," Corrosion, Vol. 22, 1966, p. 16.
39. W. D. France and N. D. Greene, "Comparison of Chemically and Electrolytically Induced Pitting Corrosion," Corrosion, Vol. 24, 1968, p. 247.

40. H. H. Uhlig, "Pitting of Stainless Steels," American Institute of Mining and Metallurgical Engineers, Transactions, Vol. 140, 1940, p. 411.
41. M. J. Pryor, "Corrosion of Steel in Dilute Solutions of Sodium Salts of Weak Acids," Corrosion, Vol. 9, 1953, p. 467.
42. F. C. Porter and S. E. Hadden, "Corrosion of Aluminum in Supply Waters," Journal of Applied Chemistry (London), Vol. 3, 1953, p. 385.
43. N. D. Greene and M. G. Fontana, "An Electrochemical Study of Pit Corrosion in Stainless Steels," Corrosion, Vol. 15, 1959, p. 32t.
44. W. A. Wissler, "Cobalt Alloys," in Corrosion Handbook, ed. H. H. Uhlig, J. Wiley, London (1948).
45. R. V. Skold and T. E. Larson, "Measurement of Instantaneous Corrosion Rate by Means of Polarization Data," Corrosion, 1952, p. 13.
46. D. A. Jones and N. D. Greene, "Electrochemical Measurement of Low Corrosion Rates," Corrosion, 72, 1966, p. 198.
47. K.J. Vetter, "Das Elektrische Feld Innerhalb der Passivschicht des Eisens," Z. Elektrochem., 58, 1954, p. 230.
48. N. D. Greene, "Experimental Electrode Kinetics," R.P.I., Troy, New York, 1965.
49. Han Chang Shih, "The Corrosion of Surgical Implant Alloys," M.I.T. Metallurgical Engineer Thesis, August 28, 1969.
50. ASTM Standards, (F75) 7, Part 7, March, 1968, p. 958.
51. S. Rideout, W. D. Manly, E. L. Kamen, B. S. Lement, and Paul A. Beck, "Intermediate Phases in Ternary Alloy Systems of Transition Elements," Journal of Metals, Oct. 1951, p. 872.

Figure 1

EFFECT OF COBALT CONTENT ON TRANSFORMATION TEMPERATURE
OF Co-Ni-20Cr-10Mo ALLOYS

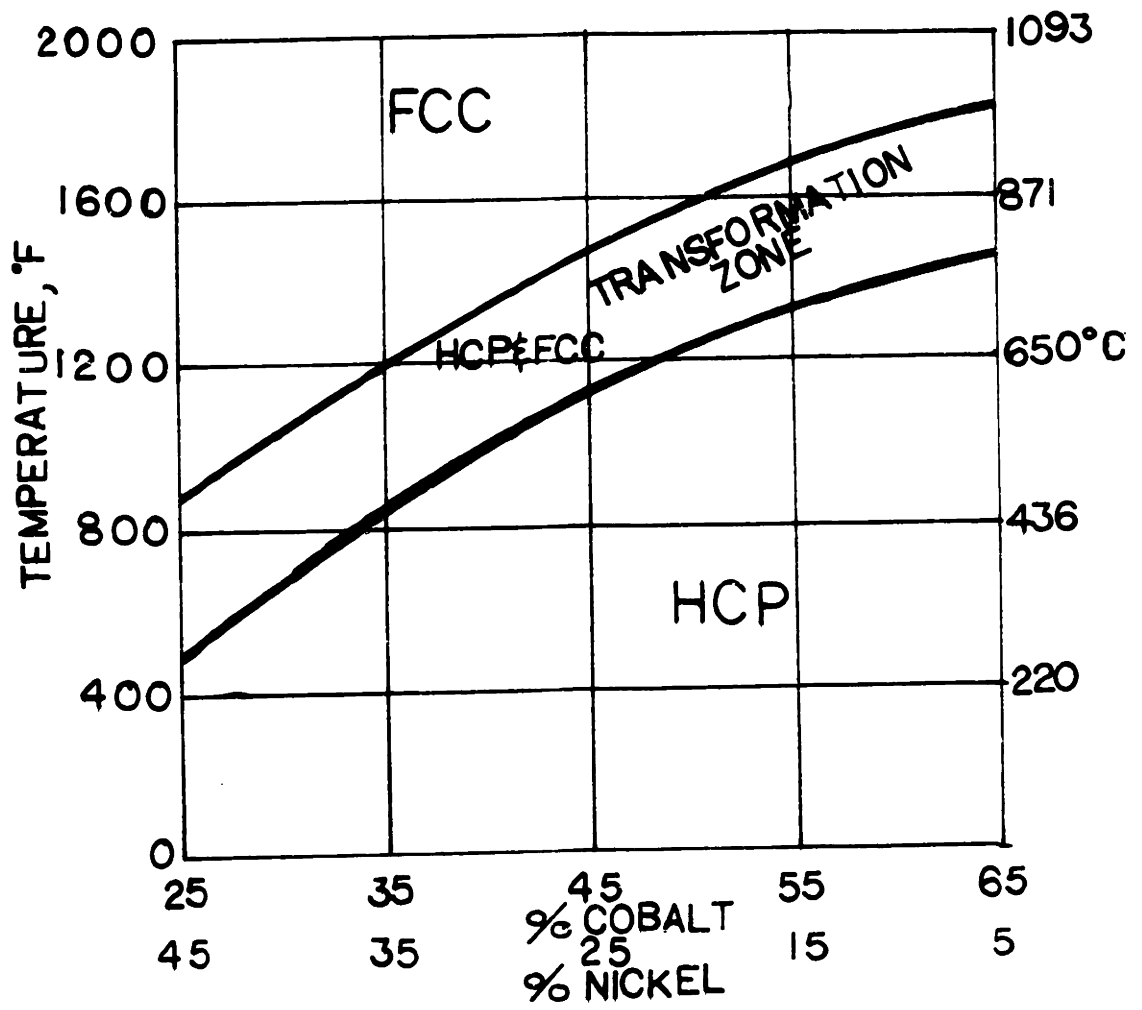
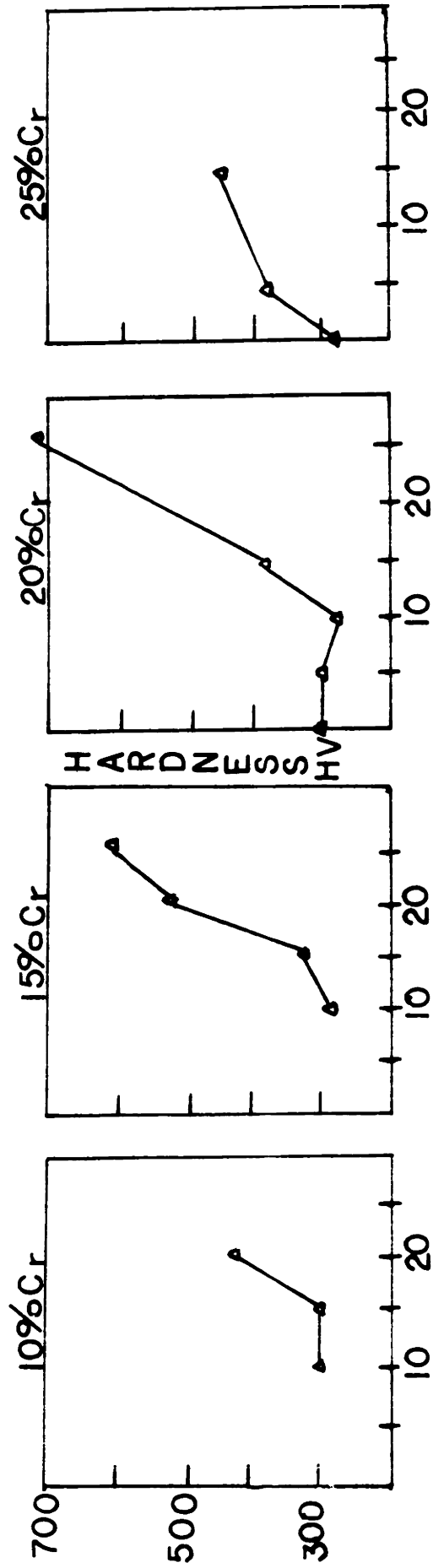


Figure 2

HARDNESS OF Co-Cr-Mo ALLOYS AFTER HEAT TREATING
FOR 10 HOURS AT 700°C



AGE FOR 10 HRS. AT 700°C

WT. % MOLYBDENUM

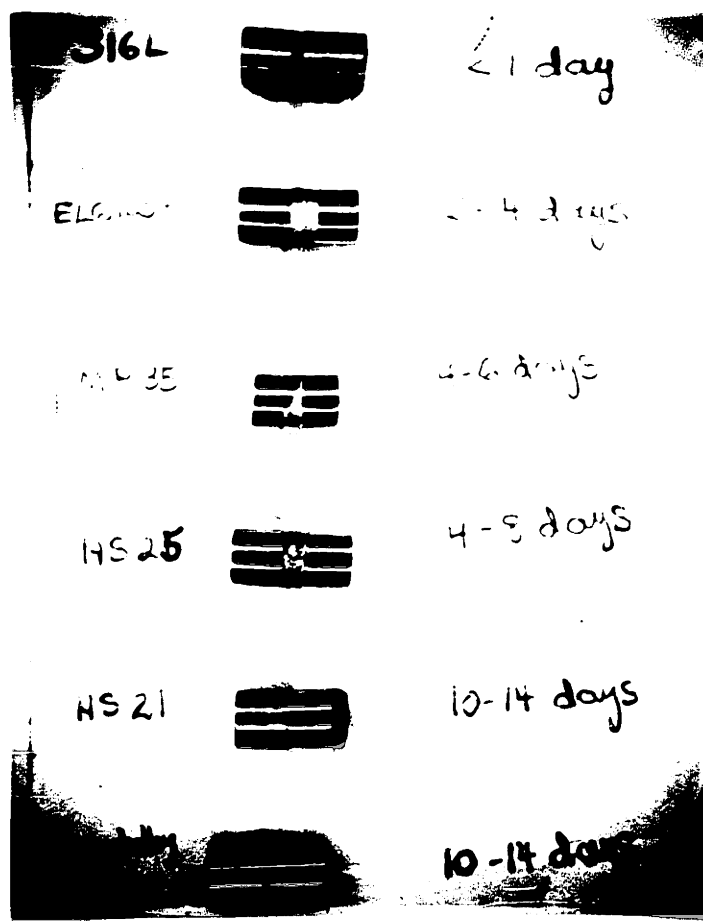


Figure 3 Crevice Corrosion Samples of Several Alloys after Immersion
in 10% HCl + 1% FeCl₃ Solution.

Figure 4

PASSIVE CURRENT DENSITY VS. TIME CURVE OF 316L STAINLESS STEEL
IN 0.9% NaCl SOLUTION

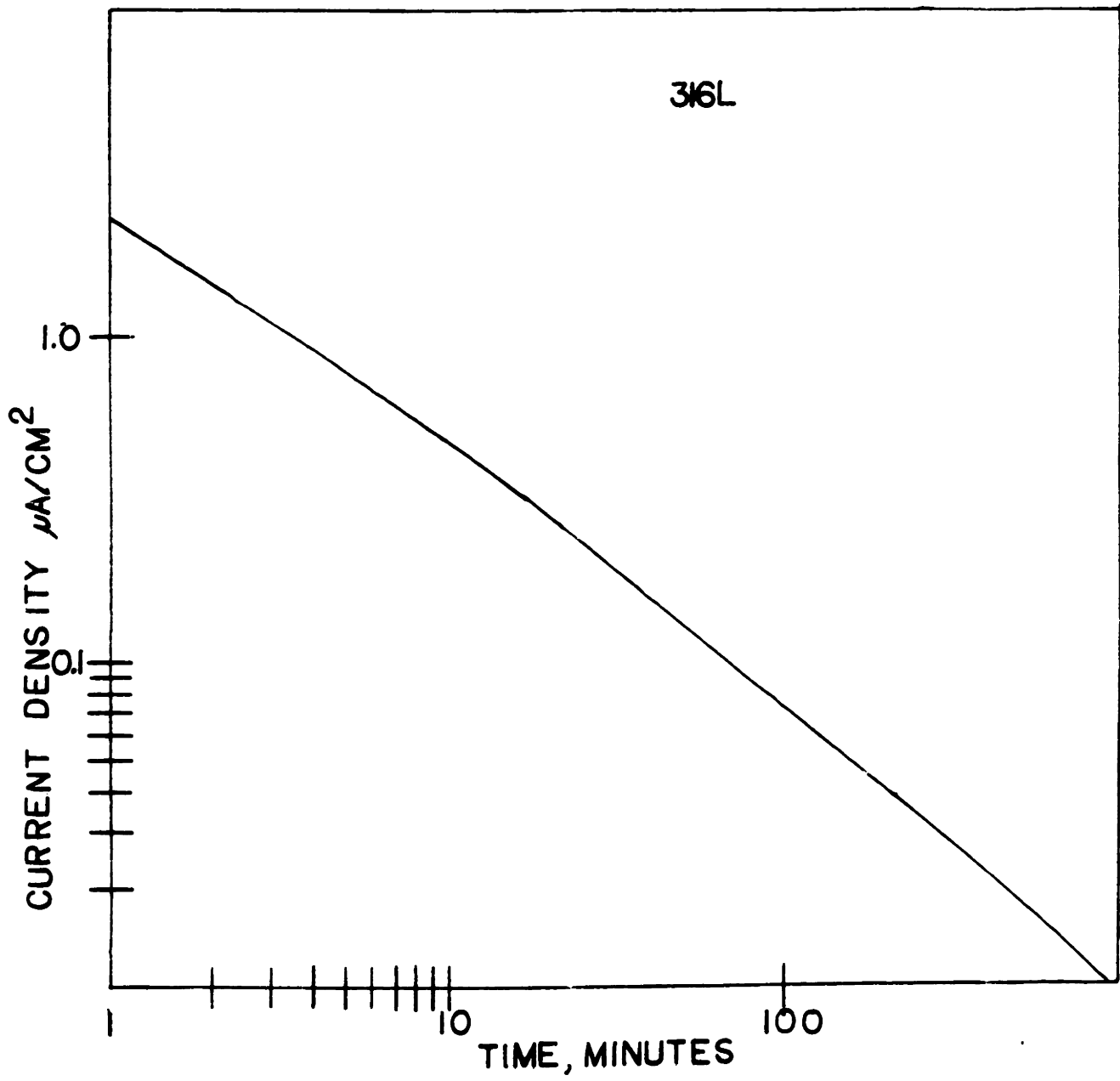


Figure 5

PASSIVE CURRENT DENSITY VS. TIME CURVE OF HASTALLOY C
IN 0.9% NaCl SOLUTION

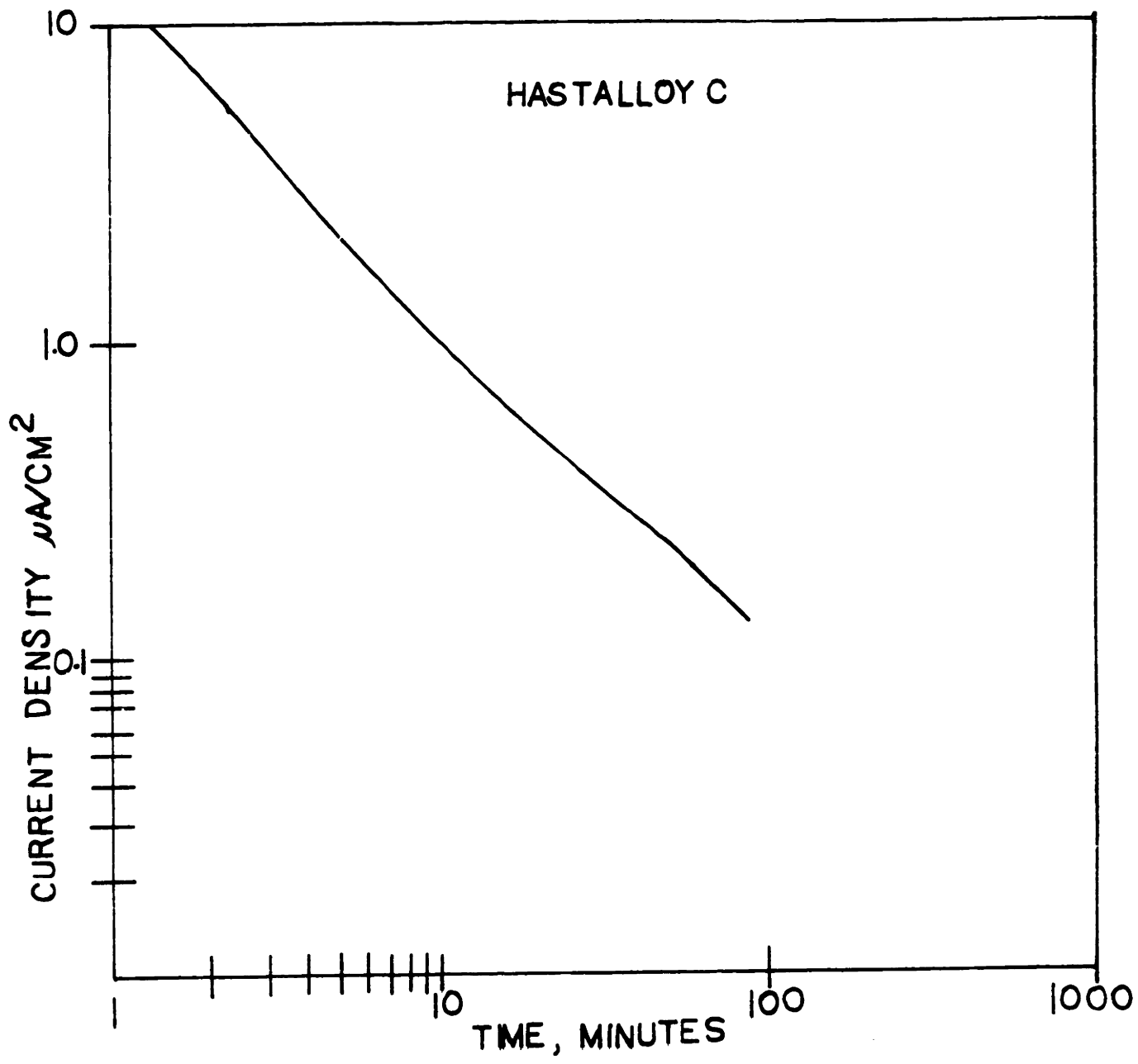


Figure 6

PASSIVE CURRENT DENSITY VS. TIME CURVE OF MP35N
IN 0.9% NaCl SOLUTION

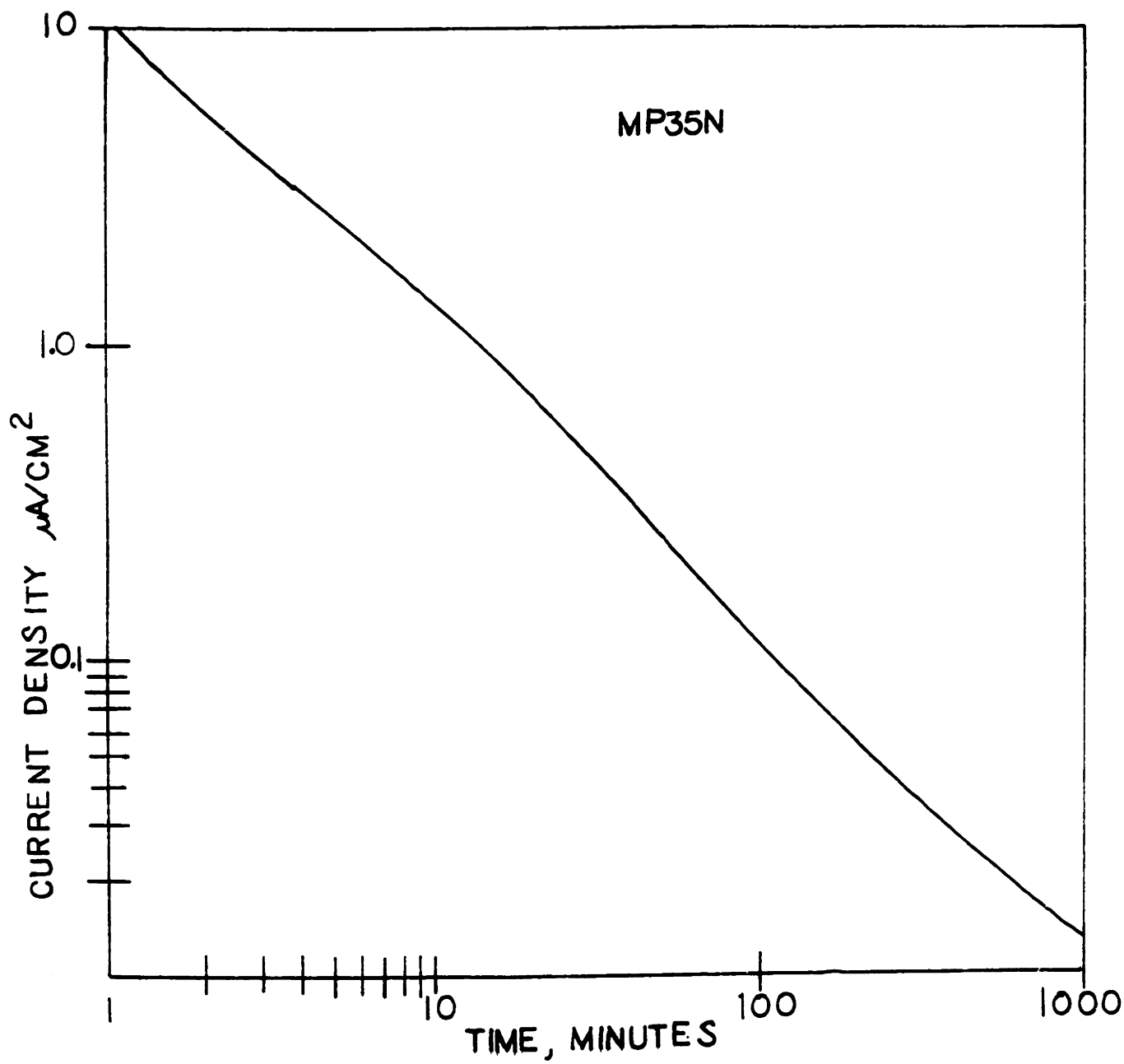


Figure 7

PASSIVE CURRENT DENSITY VS. TIME CURVE OF
HAYNES STELLITE 25 IN 0.9% NaCl SOLUTION

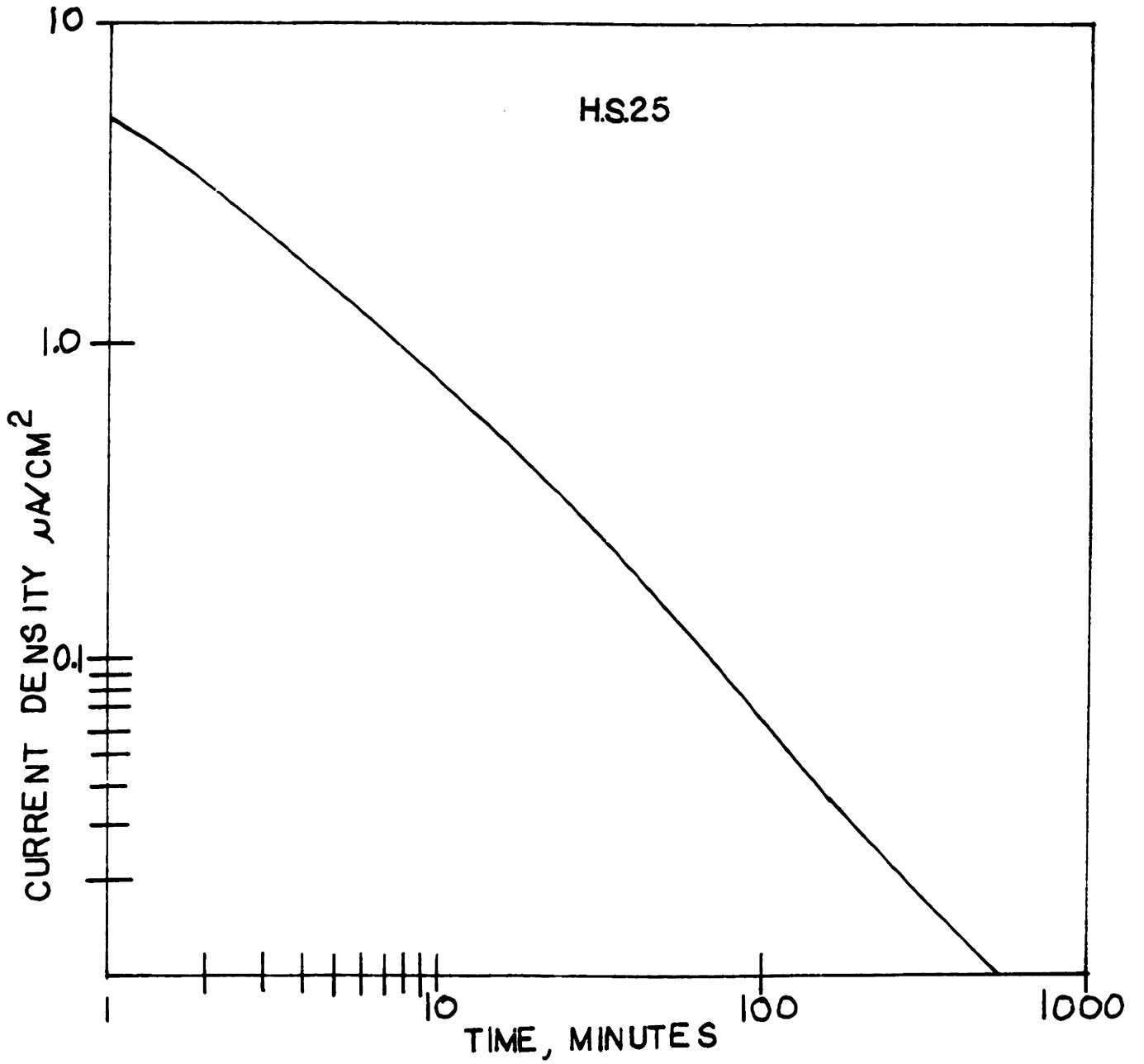


Figure 8

PASSIVE CURRENT DENSITY VS. TIME CURVE OF
HAYNES STELLITE 21 IN 0.9% NaCl SOLUTION

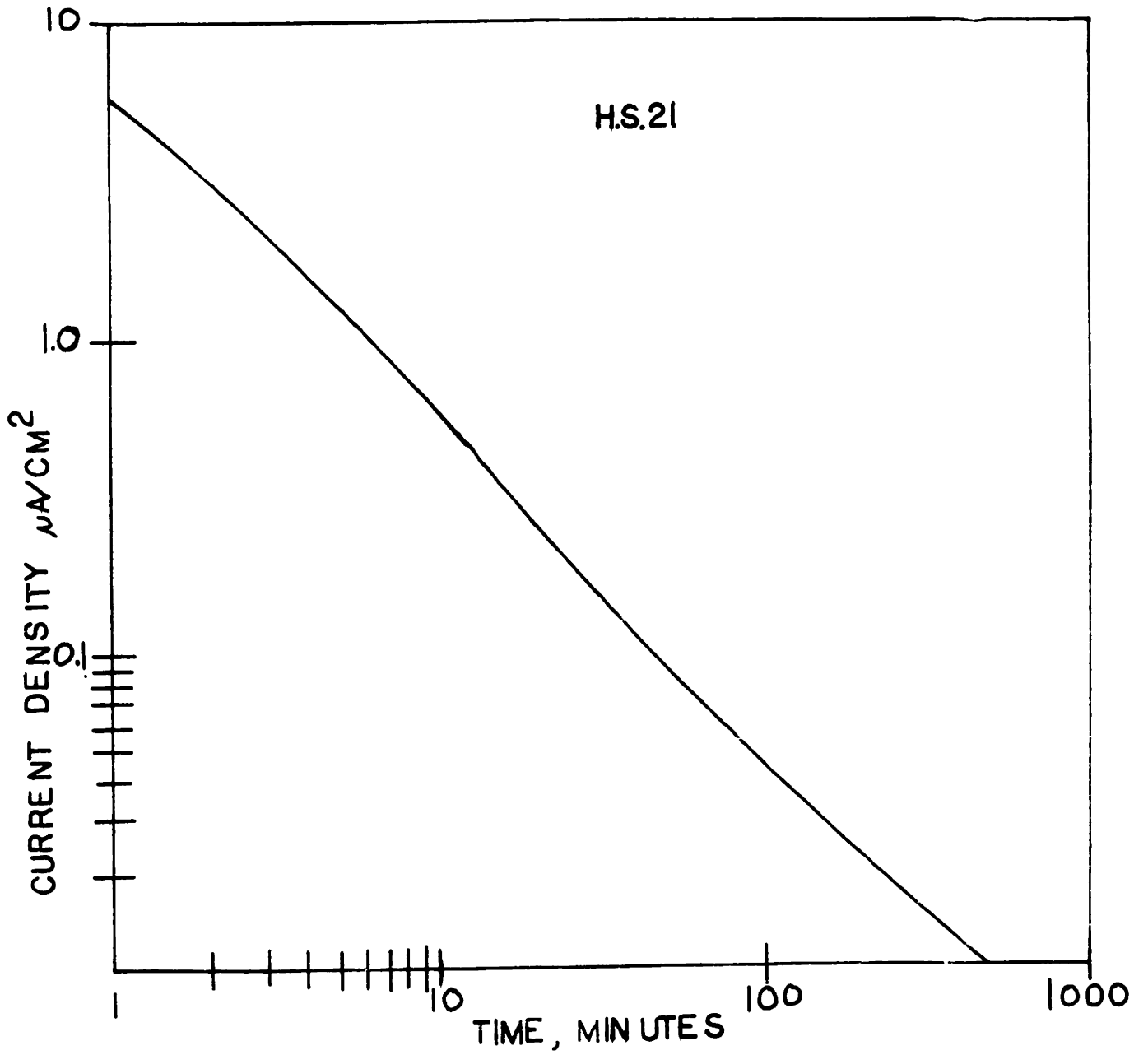


Figure 9

PASSIVE CURRENT DENSITY VS. TIME CURVE OF
M.I.T. ALLOY NO. 7 IN 0.9% NaCl SOLUTION

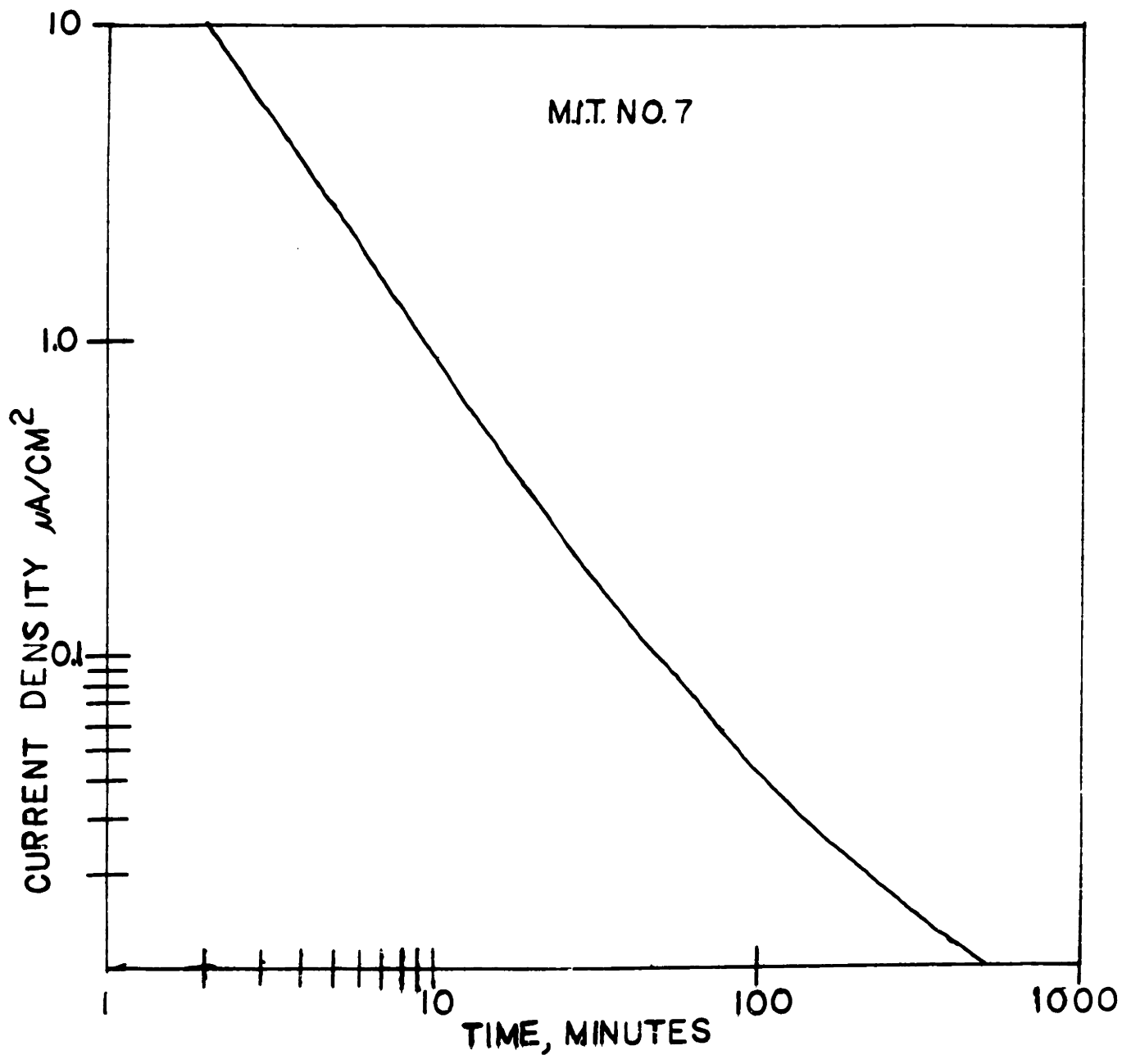


Figure 10

COMPARISON OF THE PASSIVE CURRENT VS. TIME CURVES OF
HAYNES STELLITE 21, HAYNES STELLITE 25, AND M.I.T. ALLOY NO. 7
IN 0.9% NaCl Solution

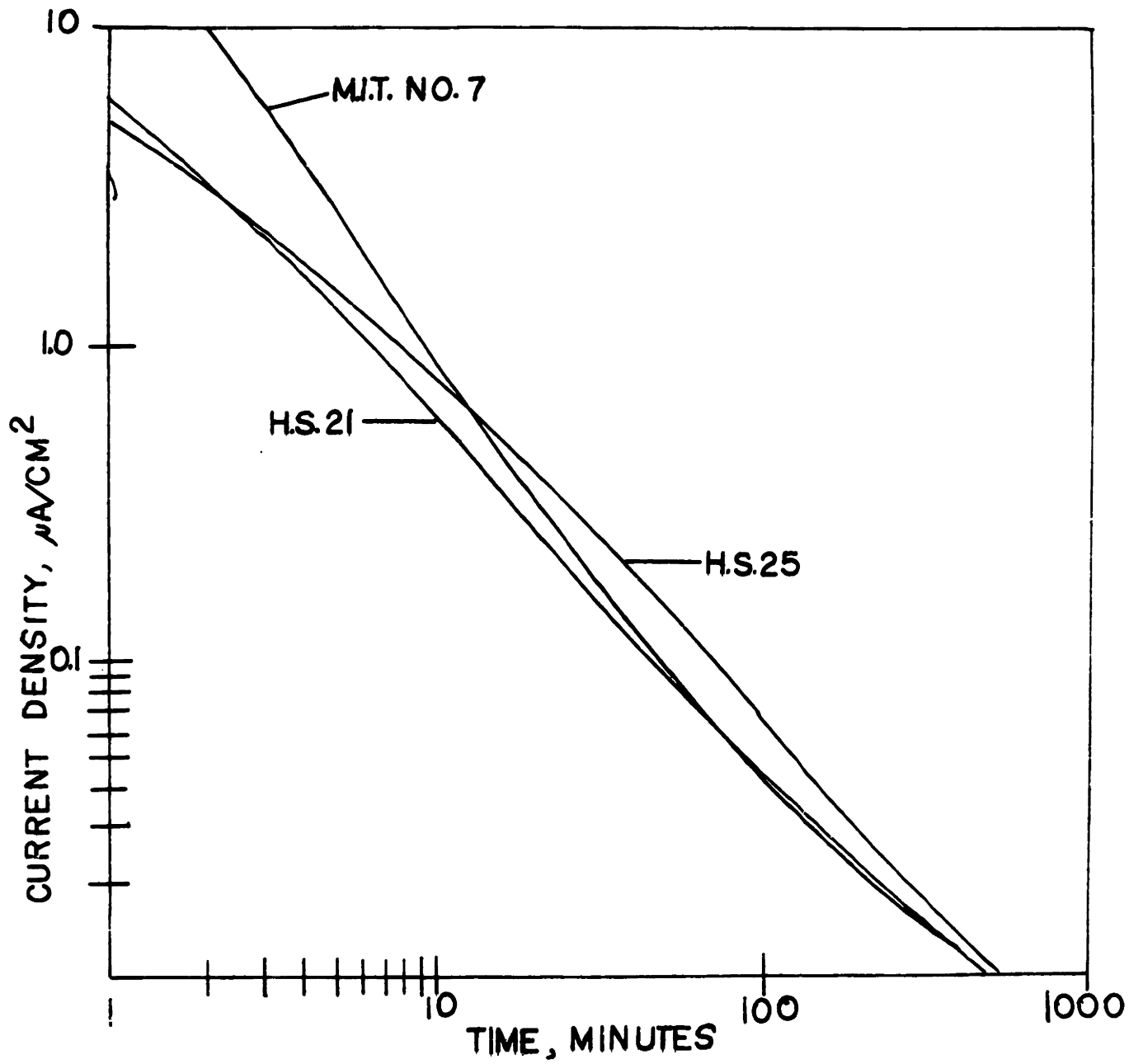


Figure 11

ANODIC POLARIZATION OF 316L STAINLESS STEEL
IN 0.9% NaCl SOLUTION

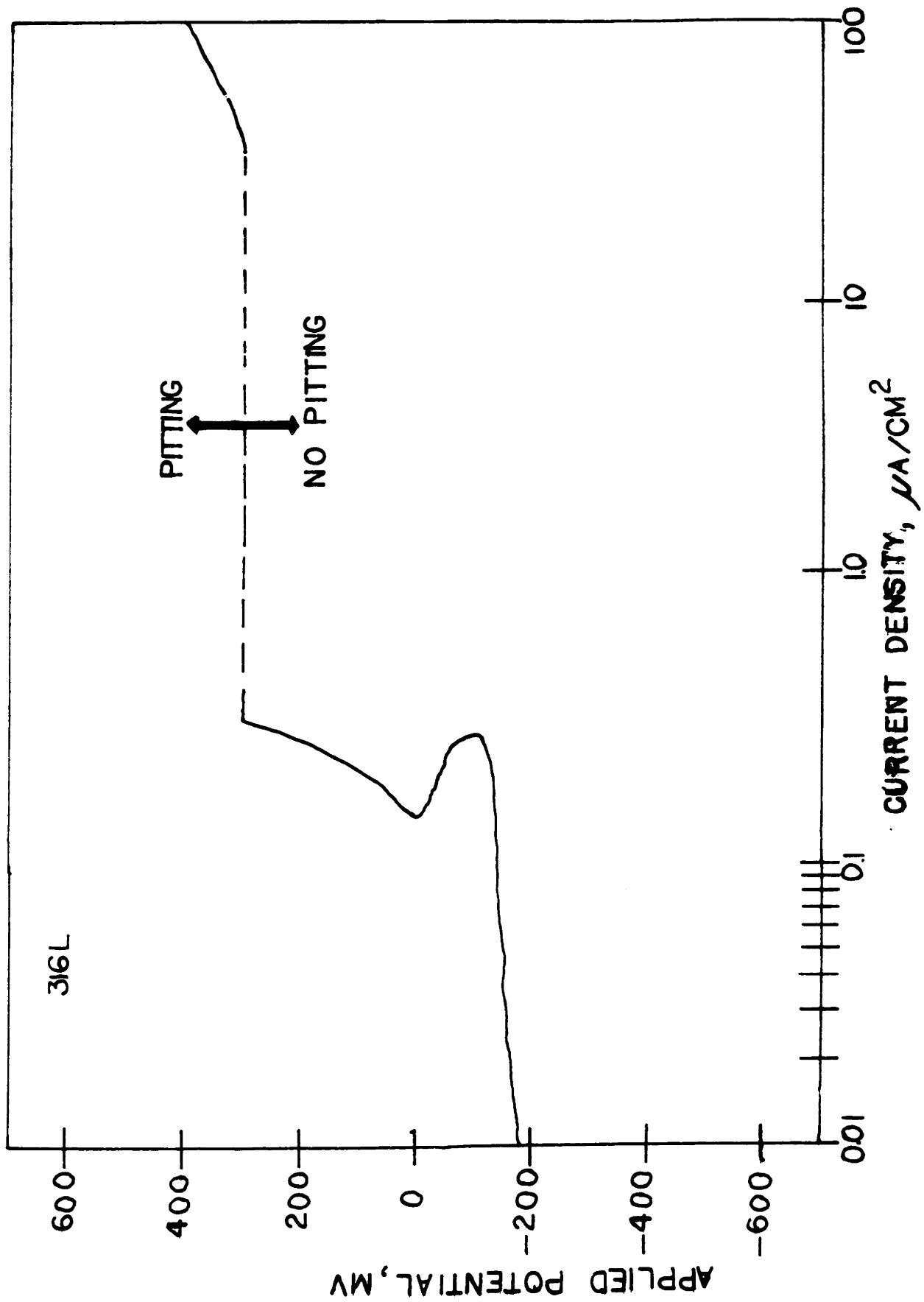


FIGURE 12

ANODIC POLARIZATION OF HASTALLOY C
IN 0.9% NaCl SOLUTION

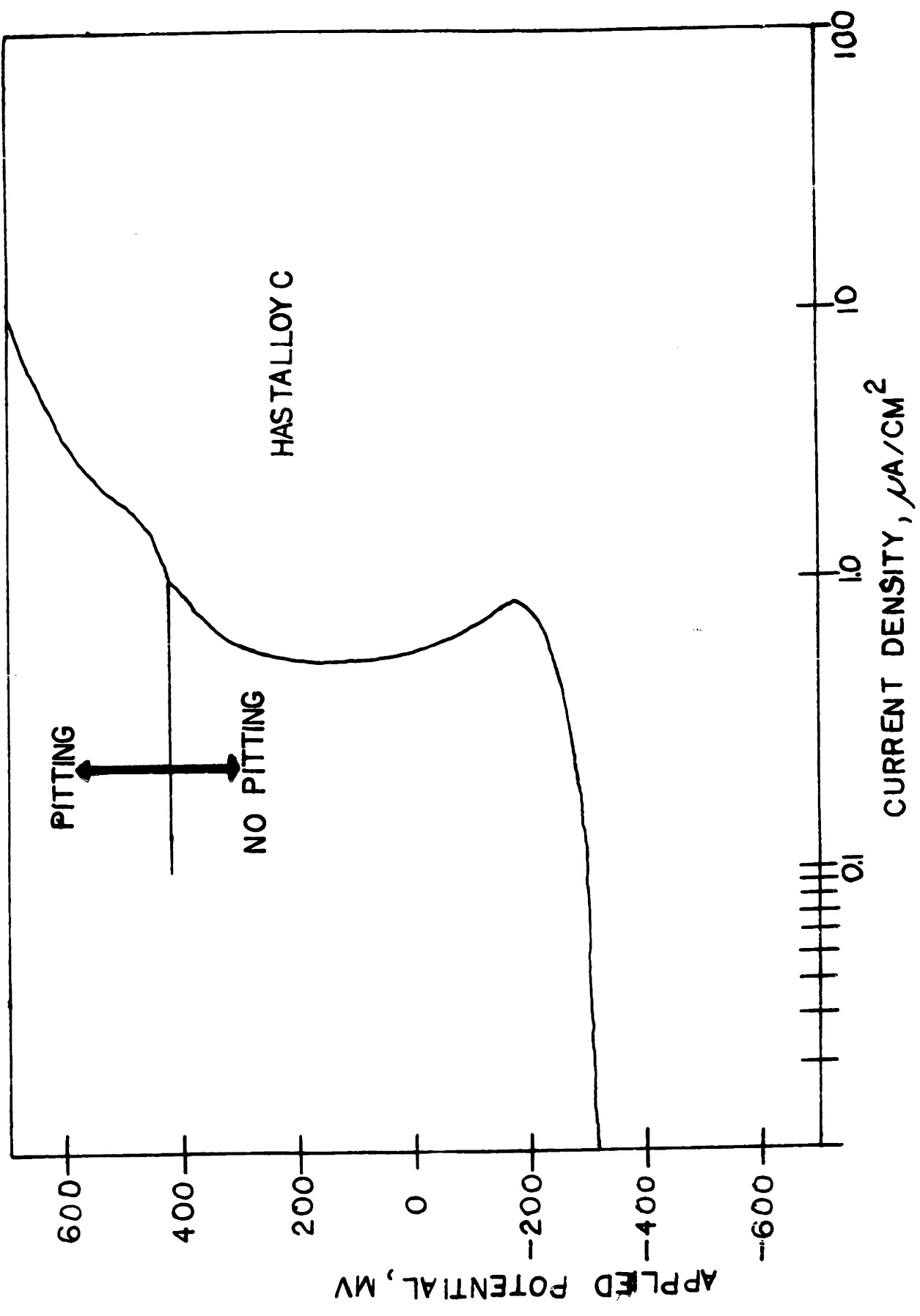


Table 13

ANODIC POLARIZATION OF MP35N IN 0.9% NaCl SOLUTION

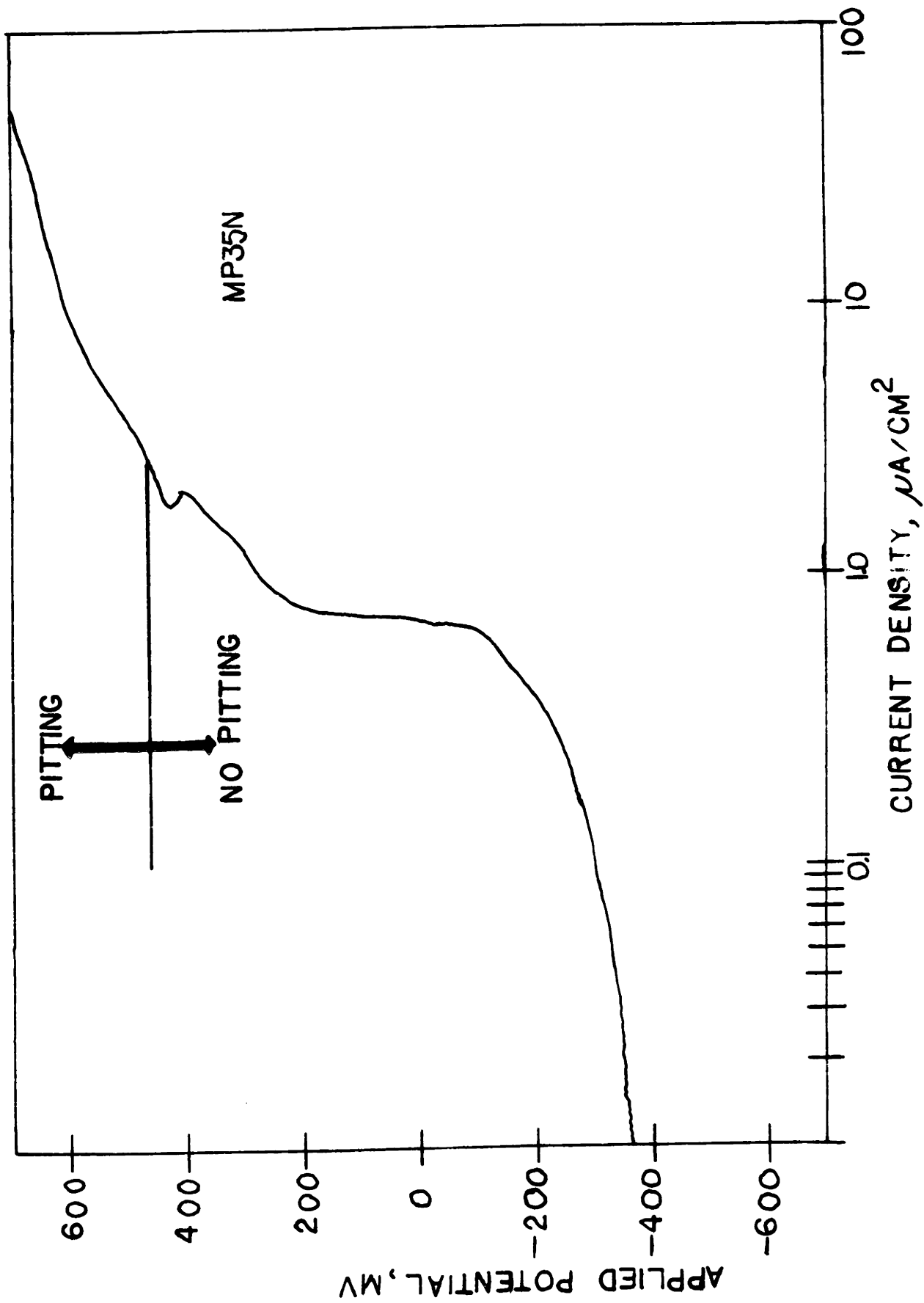


Figure 14

ANODIC POLARIZATION OF HAYNES STELLITE 25 IN 0.9% NaCl SOLUTION

Figure 14

ANODIC POLARIZATION OF HAYNES STELLITE 25 IN 0.9% NaCl SOLUTION

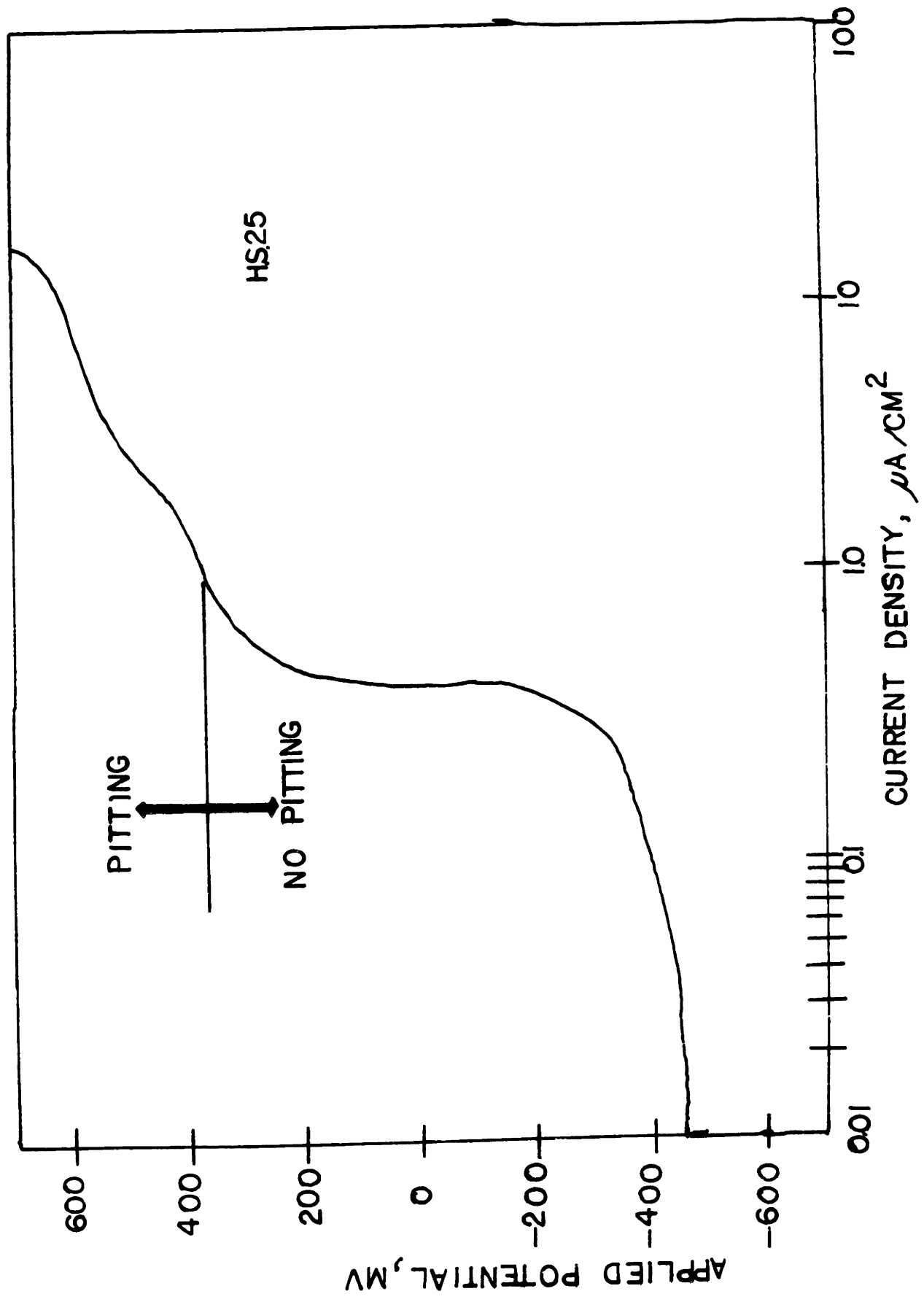


FIGURE 15

ANODIC POLARIZATION OF HAYNES STELLITE 21 IN 0.9% NaCl SOLUTION

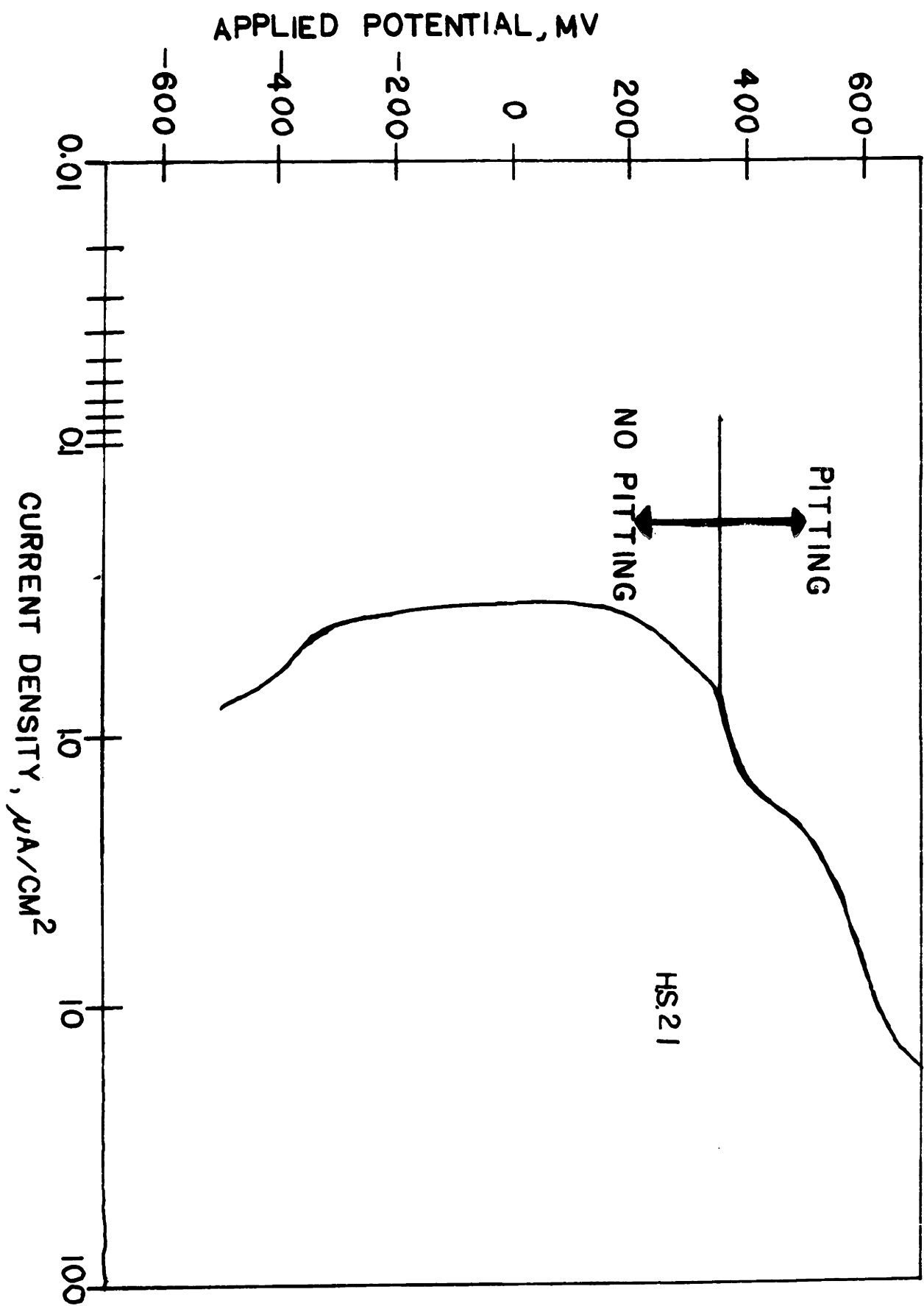


Figure 16

**ANODIC POLARIZATION OF PRECISION CAST VITALLIUM
IN 0.9% NaCl SOLUTION**

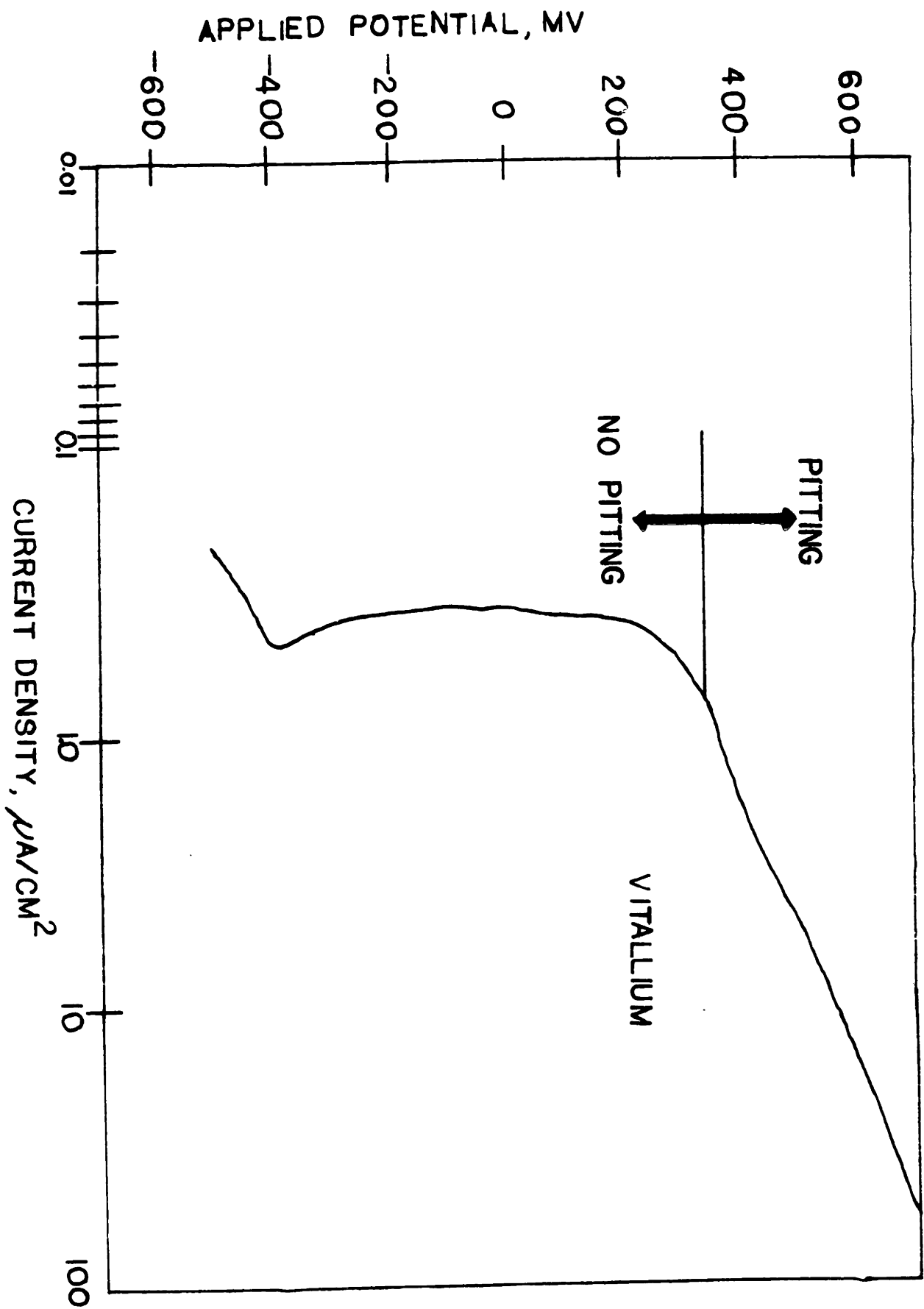


Figure 17

ANODIC POLARIZATION OF M.I.T. ALLOY NO. 7
IN 0.9% NaCl SOLUTION

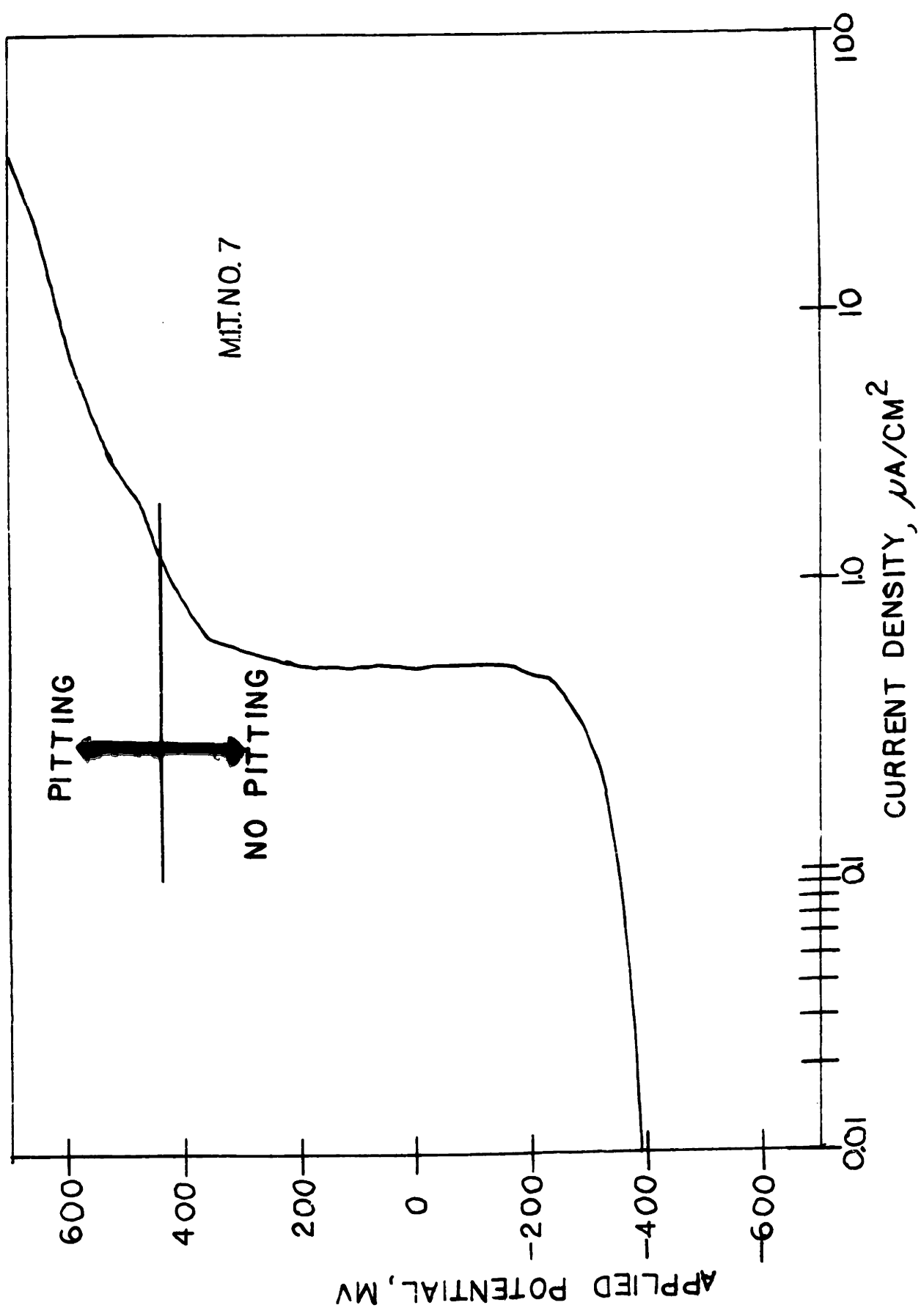


Figure 18

REST POTENTIALS OF M.I.T. ALLOY NO. 7 AND HAYNES STELLITES 21 AND 25
AFTER A 20 HOUR IMMERSION IN 0.9% NaCl SOLUTION

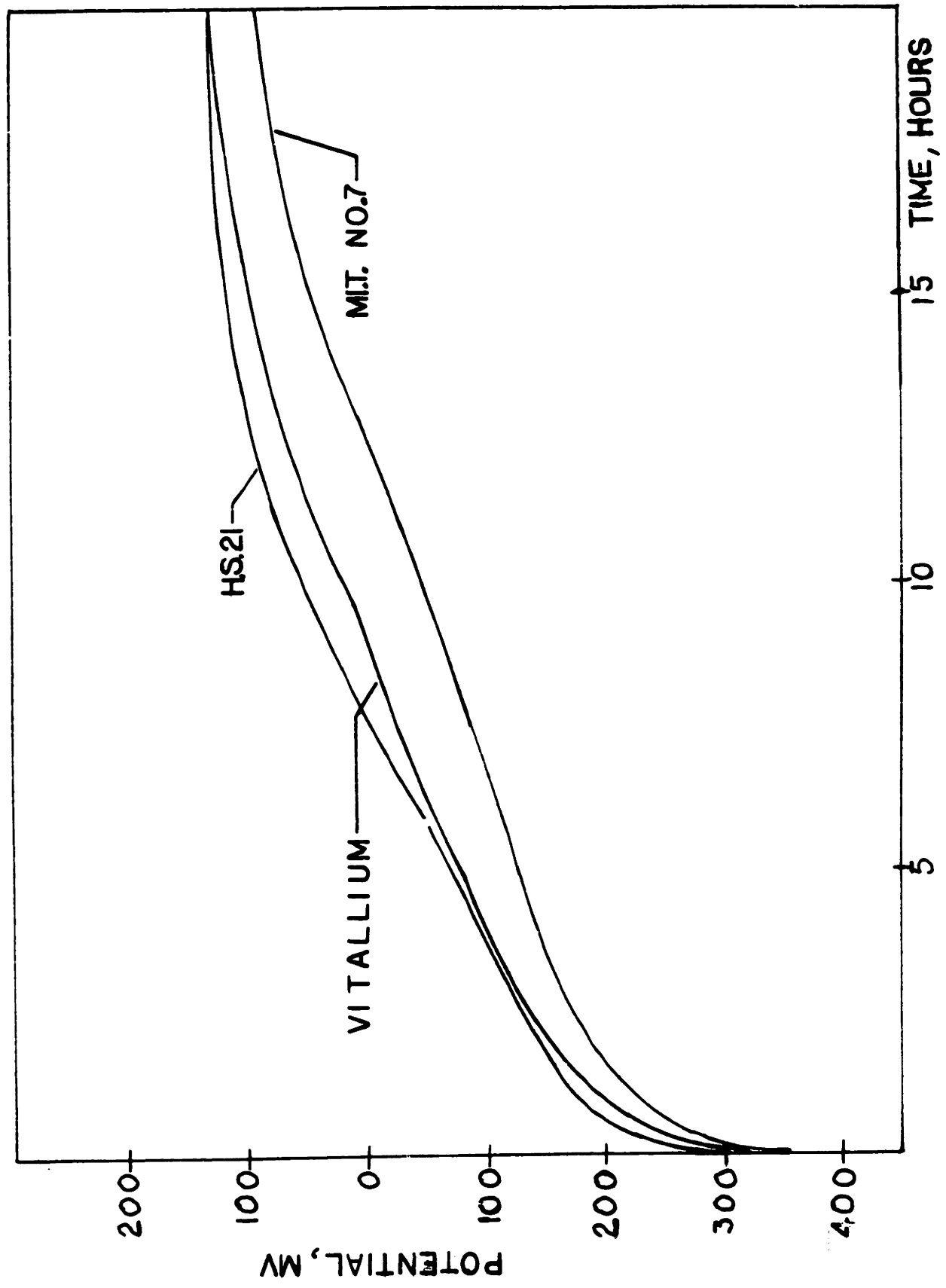




Figure 19 M.I.T. Alloy NO. 7. Annealed at 1200°C for 4 Hours. and Quenched in Water. 5% HCl Electrolytic Etch. X500.



Figure 20 M.I.T. Alloy No. 7. Directionally Solidified and Extruded.
5% HCl Electrolytic Etch. X500.



Figure 21 M.I.T. Alloy No. 7. Hot and Cold Worked and Heat Treated.
at 1100°C for 1 Hour and Quenched in Water. 5% HCl
Electrolytic Etch. X500.

Table 1

NOMINAL COMPOSITIONS OF SURGICAL IMPLANT ALLOYS

	<u>Cr</u>	<u>Mo</u>	<u>W</u>	<u>Ni</u>	<u>C</u>	<u>Fe</u>	<u>Co</u>	<u>Ti</u>	<u>Other</u>
316	16 - 18	2 - 3	---	10 - 14	<0.08	Bal	---	---	<2Mn <1Si
316L	17 - 20	2 - 4	---	10 - 14	<0.03	Bal	---	---	<2Mn <.75Si
H.S.25	19 - 21	---	14 - 16	9 - 11	<0.15	<3	Bal	---	<2Mn <1Si
H.S.21	25 - 30	4.5 - 6.5	---	1.5 - 3.5	0.2 - 0.35	<2	Bal	---	<1Mn <1Si
Vinertia	31	6.5	N.S.	N.S.	0.5	N.S.	Bal	---	
Vitalium	30.8	5.0	---	---	0.4	0.7	Bal	---	0.5Mn 0.3Si
Titanium	---	---	---	---	0.023	0.10	---	Bal	

N.S.: Not Specified

Table 2

MECHANICAL PROPERTIES OF SURGICAL IMPLANT ALLOYS

	<u>Form</u>	<u>Yield Strength ksi</u>	<u>Ultimate Tensile Strength, ksi</u>	<u>Elongation, Percent</u>	<u>Reduction in Area, Percent</u>
316L	Annealed	35	80	45	
316L	Cold Worked	125	145	15	
H.S.25	Wrought	65 - 80	145 - 165	35	
H.S.21	Precision Casting	82	103	8	9
Vinertia	Cast	50	90	2.5	
Titanium	Annealed	40	50	22	35

Table 3
STRENGTH AND DUCTILITY OF Co-BASE Cr-Mo ALLOYS AT 1700°F

	<u>Yield Strength, ksi</u>	<u>Reduction in Area, Percent</u>
15 Cr	15	35
15 Cr - 10 Mo	50	20
15 Cr - 15 Mo	56	5
20 Cr	20	40
20 Cr - 5 Mo	38	26
20 Cr - 10 Mo	47	3
20 Cr - 15 Mo	79.4	1.5
25 Cr - 10 Mo	75	7
30 Cr - 5 Mo	51	3

Table 4

ROOM TEMPERATURE DUCTILITY OF Co-BASE Cr-Mo ALLOYS

	<u>Reduction in Area, Percent</u>
15 Cr	20
15 Cr - 10 Mo	12
15 Cr - 15 Mo	1
20 Cr	26
20 Cr - 5 Mo	30
20 Cr - 10 Mo	14
20 Cr - 15 Mo	2

Table 5

NOMINAL COMPOSITIONS OF SOME COMMERCIALY AVAILABLE WROUGHT ALLOYS,

HAYNES STELLITE 21, AND VITALIUM

	<u>Cr</u>	<u>Mo</u>	<u>W</u>	<u>Ni</u>	<u>C</u>	<u>Fe</u>	<u>Co</u>	<u>Other</u>
316L	17 - 20	2 - 4	----	10 - 14	<0.03	Bal	----	<2Mn
Elgilloy	20	7	----	15	0.15	Bal	40	<0.75Si 2Mn
MP35N	20	10	----	35	----	----	35	0.04Be ----
H.S.25	19 - 21	----	14 - 16	9 - 11	<0.15	3	Bal	< 2Mn < 1Si
Hastalloy C	13 - 17.5	16 - 18	3.7 - 5.3	Bal	----	4.5 - 7.0	----	----
H.S.21	27.5	5.5	----	2.5	0.35	2.0	Bal	1MN 0.6Si
Vitalium	30.8	5.0	----	----	0.4	0.7	Bal	0.5Mn 0.3Si

Table 6

NOMINAL COMPOSITIONS OF M.I.T. EXPERIMENTAL ALLOYS

<u>M.I.T. Alloy No.</u>	<u>Cr</u>	<u>Mo</u>	<u>Ni</u>	<u>Co</u>	<u>Other</u>
1	15	15	35	35	
2	20	10	35	35	
3	25	5	35	35	
4	20	10	20	50	
5	20	10	10	60	
6	20	10	3	Bal	
7	20	10	--	Bal	
8	25	10	--	Bal	
9	15	7.5	--	Bal	
10	19.6	3.8	--	Bal	
11	19.4	3.7	--	Bal	0.4Ta

Table 7

MECHANICAL PROPERTIES OF SOME WROUGHT COMMERCIAL ALLOYS AND H.S. 21

	<u>Condition</u>	<u>Yield Strength ksi</u>	<u>Ultimate Tensile Strength, ksi</u>	<u>Elongation, Percent</u>	<u>Reduction In Area, Percent</u>	<u>Rockwell Hardness</u>
316L	Annealed	35	80	45		B-80
	Cold Worked	125	145	15		C-33
Elgilloy	Heat Treated	280	368	17		C-58
		225	260	15	25	
MP35N	Cold Worked	225	260	15	25	
H.S. 25	Wrought	78	155	35		B-95
H.S. 21	Precision Cast	82	101	8		C-30

Table 8
SPECIFICATIONS OF MECHANICAL PROPERTIES OF
SURGICAL IMPLANT ALLOYS

Minimum Tensile Strength	95 ksi
Minimum Yield Strength (0.2% offset)	65 ksi
Minimum Elongation	8 percent
Minimum Reduction in Area	8 percent

Table 9

TIMES TO INITIATE CREVICE CORROSION OF SOME COMMERCIAL WROUGHT ALLOYS,
H.S.21, AND VITALLIUM IN A 10% HCl + 1% FeCl₃ SOLUTION AT 37°C

	<u>Processing Treatment</u>	<u>Time for Onset of Visible Crevice Corrosion</u>
316L	Annealed	2 - 10 minutes
Elgilloy	Heat Treated	4 - 6 days
MP35N	Wrought	5 - 8 days
H.S.25	Wrought	6 - 12 days
Hastalloy C	Wrought	10 - 18 days
H.S.21	Precision Cast	14 - 22 days
Vitallium	Precision Cast	> 280 days

Table 10
TIMES TO INITIATE CREVICE CORROSION OF M.I.T. EXPERIMENTAL
ALLOYS NOS. 1-7 IN A 10% HCl + 1% FeCl₃ SOLUTION
AT 37°C

<u>M.I.T. Alloy No.</u>	<u>Time for Onset of Visible Crevice Corrosion</u>
1	3 - 5 days
2	5 - 8 days
3	3 - 6 days
4	6 - 8 days
5	10 - 14 days
6	9 - 14 days
7	>280 days

Table II
TIMES TO INITIATE CREVICE CORROSION OF M.I.T. EXPERIMENTAL
ALLOYS NOS. 7-11 IN A 10% HCl + 1% FeCl₃ SOLUTION
AT 37°C

<u>M.I.T. Alloy No.</u>	<u>Time for Onset of Visible Crevice Corrosion</u>
7	>280 days
8	>280 days
9	< 10 days
10	< 10 days
11	< 10 days

Table 12

BREAKDOWN POTENTIALS IN 0.9% NaCl SOLUTION AND REST POTENTIALSAFTER A 20 HR. IMMERSION IN 0.9% NaCl SOLUTION OFH.S. 21, VITALLIUM, AND M.I.T. ALLOY NO. 7

	<u>ϕ_{BD}, mV</u>	<u>ϕ_R (20 Hr), mV</u>	<u>$\phi_{BD} - \phi_R$ (20 Hr), mV</u>
H.S. 21	360	130	230
Vitallium	340	130	210
M.I.T. Alloy No. 7	440	95	345

Table 13
HOT AND COLD WORKABILITY OF M.I.T. ALLOY NO. 7

A. Hot Working

<u>Process</u>	<u>Reduction in Area, Percent</u>
Extrusion	64
Press Forging	83
Rolling	64

B. Cold Working

<u>Process</u>	<u>Previous Treatment</u>	<u>Reduction in Area, Percent</u>
Rolling	Hot Worked	25
	Annealed	30
Swaging	Hot Worked	25
	Annealed	30

Table 14

COMPARISON OF THE ROOM TEMPERATURE TENSILE PROPERTIES OF M.I.T. ALLOY NO. 7
FOLLOWING DIFFERENT TREATMENTS WITH THOSE OF H.S. 21 AND H.S. 25

M.I.T.
 Alloy No. 7

<u>Treatment</u>	<u>Yield Strength, ksi</u>	<u>Ultimate Tensile Strength, ksi</u>	<u>Elongation, Percent</u>	<u>Reduction In Area, Percent</u>
Annealed 1200°C for 4 hrs., quenched	45.0	58.3	20	26
Aged 800°C for 4 hrs., quenched	55.2	115.1	10	12
Annealed 1200°C for 4 hrs., quenched and cold swaged at 25%RA	94.4	138.2	<2	2
Directionally Solidified and Extruded	110.3	133.8	5.2	16
Directionally Solidified, and Extruded, and Aged at 900°C for 1/2 hr.	117.4	134.0	6.5	19

Table 14 (Cont.)

<u>Treatment</u>	<u>Yield Strength, ksi</u>	<u>Ultimate Tensile Strength, ksi</u>	<u>Elongation, Percent</u>	<u>Reduction In Area, Percent</u>
Directionally Solidified, Extruded, aged for 1 hr. at 1000°C, quenched and then aged for 1 hr. at 1100°C	72.3	141.6	9	38
Press Forged (83%RA), Hot Rolled (64%RA), Cold Swaged (25%RA), and aged for 1 hr. at 1100°C	125	206	25	26
H.S. 21 Precision Cast	82	101	8	
H.S. 25 Wrought	70	150	65	